DELFT UNIVERSITY OF TECHNOLOGY
Faculty of Electrical Engineering
Telecommunications and Traffic
Control Systems Group

Title: The reliability of carrier phase DGPS position solutions in a high-dynamical environment.

The truth reference, the whole truth reference and nothing but the truth reference?

Author: R.A. Gutteling

Nature of report: Thesis Report
No. of pages: 74
Date: August 1996

Professor:	Prof. dr. ir. D. van Willigen
Mentors:	ir. E.J. Breeuwer
	ir. S.P. van Goor
	ir. M.B. Zaaijer
Assignment no.:	A-712
Period:	june 1995 - august 1996

In this report, some tests are described which have been used to determine the reliability of carrier-phase DGPS position solutions, especially in a dynamical environment, such as an aircraft. Research has been done to determine the reliability of the acceptance test, used to determine whether a carrier-phase DGPS position solution is the 'true' position. The results of this research are presented in this report.

Keywords: DGPS, carrier-phase, truth reference, ratio-test

Preface

This report is the result of my thesis work. It is the conclusion of the research I did for the MIAS-project.

In order to be able to understand the contents of this report, some knowledge of electronics and satellite navigation is required. If you are reading this report without knowledge of satellite navigation, reading the chapters 2 and 3 is recommended in order to understand the (im)possibilities and applications of satellite navigation systems and the way a position solution is calculated.

If you are only interested in the conclusions of my research, it is recommended to read chapters 4, 5 and 6, which lead to the conclusions of chapter 7.

I would like to thank the following persons (in no particular order) for their help and support:

- The staff of the Scheepvaart en Transportcollege "Professor Rutten" for making the harbour crane test possible;
- mr. J. Zomerdijk of the Meetkundige Dienst for his help with the post-processing software;
- ir. C. Tiberius of the faculty of Geodetic Engineering for his explanation of the different DGPS carrier-phase ambiguity resolution techniques;
- the staff of the Delft University of Technology Sportcentrum, for their permission to (temporarily) place a reference antenna on one of the hockey-fields;
- mr. A. Plooster for his help during the second turntable test and his help with the video presentation;
- the staff and students of the P&N group for their support and companionship, especially ir. M.B. Zaaijer for his help during the harbour crane test, ir. E.J. Breeuwer for his assistance during my entire thesis project and prof. dr. ir. D. van Willigen for his support and useful comments during the final phase of writing my thesis report.

Summary

Requirements on aircraft navigation systems are continuously increasing. Important aspects are accuracy, reliability and integrity. To be able to meet the requirements, existing systems have to be modified or new systems need to be developed.

A new system that might meet all the requirements within a few years is called MIAS (*M*ulti-mode *I*ntegrated *A*pproach *S*ystem). MIAS is a combination of the world-wide satellite navigation system GPS and MLS (*M*icrowave *L*anding *S*ystem), a runway-fixed navigation system that may be used during the final part of a flight.

At the faculty of Electrical Engineering of the Delft University of Technology, research is done to determine the usefulness of MIAS, especially the accuracy of the combination of MLS and GPS. For this purpose, there have been some test flights to test the MIAS system. During post-processing in the laboratory, the calculated MIAS position is compared to a reference position based on carrier-phase DGPS, which is computed using raw GPS data gathered in the aircraft and raw GPS data gathered at a reference station on the ground. This position reference is usually referred to as 'truth reference'.

To get an indication of the reliability of this carrier-phase based truth reference, the so-called 'ratio test' is used. When the value of this test exceeds a pre-set threshold value, the truth reference is assumed to be the true position. However, the question remains about what will be a 'good' threshold value.

During the research, of which this report is the result, it has been investigated whether the threshold value of 2, used by the post-processing software 'Geotracer' for its decision about the correctness of a calculated position solution, always results in the 'right' position. This turns out not to be the case; when a position solution is calculated a few times in a row using the same dataset but a different starting time within the dataset, differences in position solutions are possible, in spite of a ratio test value which in all cases was larger than the threshold value. The differences can be as much as 6 wave-lengths, approximately 120 centimetres, for an identical part of the test data, dependent on the starting time. It has to be pointed out that the differences occurred when the value of the ratio test only just exceeded the threshold value. In theory, the difference in position solutions could be eliminated by raising the threshold value. This, however, increases the risk of wrongly rejecting a good position solution because its ratio test value did not exceed the (higher) threshold value.

In order to keep the truth reference a reliable position solution, the value of the ratio test should not be trusted blindly, but instead be interpreted in a sensible way.

Samenvatting (summary in Dutch)

De eisen die aan luchtvaartnavigatiemiddelen worden gesteld worden steeds strenger. Belangrijke eisen zijn onder meer nauwkeurigheid, betrouwbaarheid en integriteit. Om aan deze eisen te kunnen (blijven) voldoen, moeten bestaande systemen aangepast of nieuwe systemen ontwikkeld worden.

Een nieuw systeem, dat binnen enkele jaren aan alle eisen zou kunnen voldoen, is MIAS (*M*ulti-mode *I*ntegrated *A*pproach *S*ystem). Dit systeem wordt gevormd door een combinatie van het wereldwijde satellietnavigatiesysteem GPS en MLS (*M*icrowave *L*anding *S*ystem), een landingsbaan gebonden navigatiesysteem dat tijdens het laatste deel van een vlucht gebruikt kan worden.

Binnen de faculteit elektrotechniek van de Technische Universiteit Delft wordt onderzoek gedaan naar de bruikbaarheid van MIAS, in het bijzonder naar de nauwkeurigheid van de MLS/GPS combinatie. Om deze nauwkeurigheid te onderzoeken is een aantal vliegproeven gedaan. De door MIAS berekende positie wordt achteraf vergeleken met een op draaggolf-DGPS gebaseerde positiereferentie, die wordt berekend aan de hand van in het vliegtuig gemeten GPS data en GPS data van een referentiestation op de grond. Deze referentie wordt meestal aangeduid met de engelse term 'truth reference'.

Voor een indicatie van de betrouwbaarheid van de truth reference wordt de ratio test gebruikt. Als de uitkomst van deze test boven een bepaalde drempelwaarde ligt, wordt aangenomen dat de truth reference inderdaad de juiste positie is. Het is echter maar de vraag wat een goede drempelwaarde is.

Tijdens het onderzoek, dat in dit verslag beschreven is, is onderzocht of de drempelwaarde 2, die door het softwarepakket Geotracer gebruikt wordt bij de beslissing over de juistheid van een gevonden positie-oplossing, altijd de juiste positie oplevert. Na onderzoek blijkt dit niet het geval te zijn; als de positie een aantal keer achter elkaar uitgerekend wordt, uitgaande van dezelfde dataset maar een andere starttijd binnen die dataset, dan kan het voorkomen dat er, ondanks een ratio die in alle gevallen groter was dan de drempelwaarde, verschillen in de positiebepaling optreden. Deze verschillen

kunnen oplopen tot 6 golflengtes, ongeveer 120 centimeter, over een identiek deel van de testdata, afhankelijk van het starttijdstip. Hierbij moet wel opgemerkt worden dat de verschillen optraden bij waarden van de ratio test die dicht bij de drempelwaarde lagen. In theorie zou het positieverschil dus geëlimineerd kunnen worden door de drempelwaarde van de ratio te verhogen. Dit geeft echter wel een hogere kans op het ten onrechte niet accepteren van een goede positie-oplossing omdat de bijbehorende waarde van de ratio test onder de (hogere) drempel lag.

Voor een betrouwbare truth reference is het nodig dat er niet zomaar op de waarde van de ratio test vertrouwd wordt, maar dat de uitkomst van de ratio test op een verstandige manier geïnterpreteerd wordt.

Abbreviations and symbols

g	Acceleration of gravity; 9.80665 m/s^2
GPS	Global Positioning System
LORAN	LOng RAnge Navigation
MIAS	Multi-mode Integrated Approach System
MLS	Microwave Landing System
λ	Wavelength of the GPS L1-carrier; approx. 19.05 cm

Table of contents

1 Introduction

Requirements on aircraft navigation increase almost every day. In order to accommodate this, new or improved navigation systems need to be available. Important aspects of (new) navigation systems are *accuracy*, *reliability* and *integrity*. Any system that does not meet these requirements will never be selected as a navigation system for aircraft.

One of the systems that might meet all the requirements within a few years is the Global Positioning System (GPS), as a stand-alone system or in combination with other systems. In its original form, GPS is not accurate enough for aircraft use (only about 100 meters), but when differential corrections are used, the accuracy is highly improved. When the phase of the GPS carrier is also used, an accuracy in the order of a few centimetres for differential solutions can be achieved.

To transmit the differential corrections, necessary for DGPS measurements, to the aircraft, various methods have been developed. It is possible to use existing navigation systems for this purpose, for example LORAN-C or MLS. The combination DGPS-MLS is called MIAS (*M*ulti-mode *I*ntegrated *A*pproach *S*ystem). With MIAS, the MLS auxiliary dataword channel is used to transmit differential corrections to aircraft in the vicinity of the MLS ground station.

At the Delft University of Technology, research is done to determine the usefulness of MIAS, especially the accuracy of the combination of MLS and GPS. For this purpose, there have been some test flights to test the MIAS-system.

To validate the MIAS position solution, it is checked against a carrier-phase DGPS position solution. This solution is computed after the flight (post-processing), using the raw GPS data gathered in the aircraft and raw GPS data gathered at the reference station on the ground. The positions computed should be accurate enough to use it as the 'true flown path'. The set of computed positions is commonly referred to as 'truth reference'.

When the truth reference has been computed, a reliability-indicator is required to give an indication of the trustworthiness of the truth reference. Such an indicator exists, and is known as the 'best solution - second best solution ratio'. The idea behind this ratio test and the way the ratio is computed are covered in chapter 3.

The goals of the research, of which this report is the result, were to determine the reliability of carrier-phase DGPS positions in a high-dynamical environment and to determine whether the ratio between the best and second best solution is a reliable indication of the quality of the DGPS solution found. To be able to reach these goals, some tests have been done.

The first test was a stationary test to determine the noise on the received signal. Afterwards, two rotation tests have been done to create a controlled dynamical environment. During the first rotation test, a GPS antenna was mounted on top of the boom of a small harbour crane. For the second rotation test, a turntable has been used. The results of these three tests are compared to and supplemented with the results of some flight tests. The GPS-data gathered during all of the tests was post-processed in the laboratory to obtain a carrier-phase DGPS position solution.

This report will start with a short introduction to the different forms of GPS. Chapter 3 will cover carrier-phase positioning, followed by the influence of a dynamical environment on DGPS position solutions in chapter 4. Chapter 5 will be used to describe the tests which have been performed to determine the accuracy of carrier-phase DGPS. The results of these tests and the software used to obtain the results will be described in chapter 6, followed by the conclusions and recommendations in chapter 7.

2 An introduction to GPS

In this chapter, the different forms of the Global Positioning System (GPS) will be described. GPS is a navigation system, based on 24 earth-orbiting satellites (21 active satellites and 3 active spares). It is still a military system, although it is used more and more for civil navigation purposes.

2.1 GPS positioning

GPS is a satellite-based navigation system, which can be used around the world. The only thing needed for a position solution is a simple receiver. GPS navigation is based on simultaneous range measurements to (at least) four different satellites, in order to solve four equations with four unknown factors: latitude, longitude, altitude and time.

To enable all users to use the system worldwide, 24 hours a day, 24 satellites have been launched. These satellites are located in six orbital planes, with four satellites in each plane (fig. 2-1).

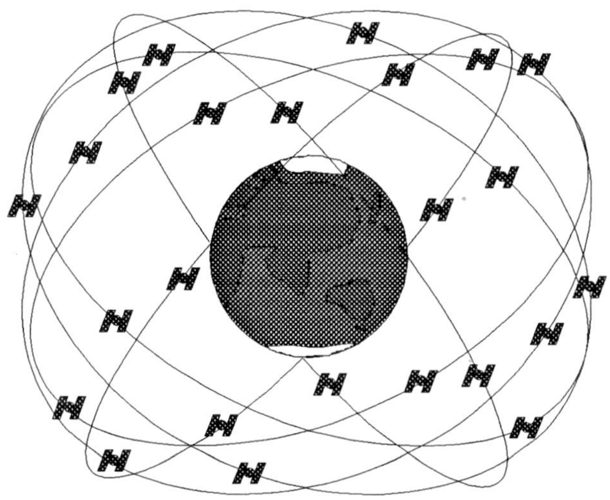

Figure 2-1 GPS Satellite orbit arrangement [1]

A GPS position fix is based on pseudorange measurements to at least four satellites. Every satellite transmits its own trajectory parameters (i.a. satellite position, clock error and health) and its local time. From the time it takes the signal to reach the GPS antenna it is possible to calculate the distance from the user to each satellite within view. From the knowledge of the trajectory parameters, it is possible to calculate the satellite position at the time of transmission. The combination of distances to the satellites and locations of the satellites will result in a unique position on Earth with an accuracy of approx. 100 meters. More information about GPS positioning can be found in [7].

2.2 Differential GPS

Although 100 meters accuracy anywhere on Earth seems very accurate, it is not accurate enough for aircraft navigation. To improve the accuracy, a GPS receiver can be placed on a strategic, exactly known, reference position, for example the end of a runway. By taking the difference between the known position of the receiver and the position calculated from the GPS signals, an error signal results, which can be transmitted to all GPS users in the vicinity of the reference receiver. The users can add this error signal to their own calculated position to obtain a much more accurate position than with GPS alone. An extra advantage of this technique is that the propagation errors due to the atmosphere are also cancelled, since these propagation errors are approximately equal for all receivers within a 20 km range from the reference station.

The error-signals, or *differential corrections* can be transmitted to all nearby users using a radio link or other, existing, navigation systems, like the microwave landing system (MLS) or LORAN-C. When the GPS differential corrections are transmitted using MLS, the combination is called MIAS (Multi-mode Integrated Approach System), when using LORAN-C, the combination is called Eurofix.

Using an existing navigation system for the transmission of the differential corrections has certain advantages over using a separate radio link. The first advantage is that there is no need to reserve frequencies in the radio spectrum, since the existing systems already use certain frequencies. The second advantage is that using an existing navigation system in combination with GPS will increase the availability and integrity of GPS, for there is a backup system in case GPS fails. The reference station will also enable a kind of 'GPS unreliable' warning, something GPS in itself is not capable of. The third advantage is that, since all the antennas needed for the reception of the differential signal are already present because of the existing navigation systems, the user has no (or very little) additional costs.

2.3 Carrier-phase DGPS

Instead of using the code-message from the satellites to calculate a position, it is also possible to use the carrier-phase. The receiver generates a carrier wave and compares it with the satellite carrier wave. From the phase difference between the locally generated carrier wave and the satellite carrier wave, accurate positioning is possible, much more accurate than positions based on code measurements. A disadvantage of carrier-phase positioning is the ambiguity, since the wavelength of the satellite carrier wave is only 19.05 cm. The phase ambiguities (the integer numbers of wave lengths between the satellites and the antenna) need to be resolved to get an accurate position. Once the phase ambiguities are resolved, very precise positioning is possible.

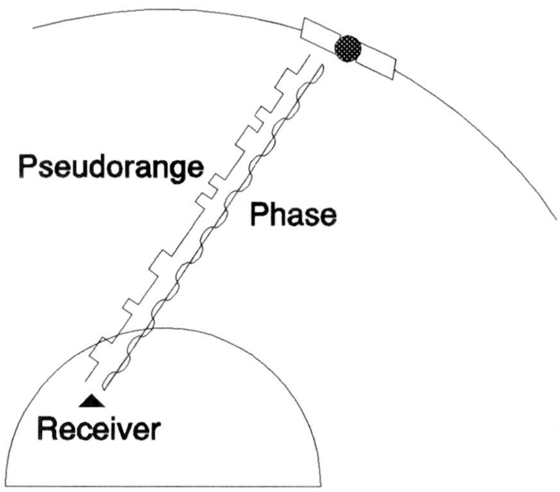

Figure 2-2 Pseudo-range and carrier phase observations [1]

A disadvantage of carrier-phase positioning is that, if initially the wrong ambiguities are found and accepted because they passed an acceptance-test, the computed position will be wrong until all of the ambiguities are recomputed, since ambiguities that are computed with the help of already computed, but incorrect, ambiguities will be incorrect themselves. An example of this can be found in chapter 5.

3 Carrier-phase positioning

The use of carrier-phase measurements for accurate GPS positioning suffers from some difficulties. The largest difficulty is to find the integer number of cycles between the receiver position and the GPS-satellites. Once those have been solved, the accurate position of the receiver can be maintained by using the Doppler-shift of the GPS carrier.

This chapter will describe the techniques used to find the integer number of cycles, needed for carrier-phase positioning, and a method to check the credibility of this number, the so-called ratio test.

3.1 Position biases

A GPS-signal normally has some biases and errors, partly due to the receiver, partly due to the satellite and partly due to the signal path. Among these biases and errors are [2]:

- receiver clock biases
- satellite clock biases
- biases due to the Earth's ionosphere
- biases due to the Earth's troposphere
- errors due to code noise
- errors due to carrier noise
- biases due to Selective Availability
- ephemerides errors
- multipath
- the integer number of cycles between the receiver and the satellites

For carrier-phase measurements, the code noise is unimportant and the carrier noise is almost equal to 0, leaving the clock biases, the ionospheric and tropospheric biases, the satellite track errors, Selective Availability, multipath and the integer number of cycles between the receiver and the satellites.

In order to eliminate (some of) these biases, different techniques have been developed. Widely known techniques are single, double and triple differences, which will be discussed in the following paragraphs.

3.2 Single differences

Generally speaking, single differences are differences between two carrier-phase measurements. They are used to eliminate one of the biases mentioned in paragraph 3.1. Single differences can be taken in three ways: between receivers, between satellites and between epochs. For carrier-phase positioning, only single differences between two receivers are used (fig. 3-1) [1].

A single difference between two receivers will eliminate propagation biases and the satellite biases (almost) entirely, depending on the distance between the receivers and the difference in height of the receivers. If the receivers are located at a different height, the tropospheric delays will not cancel out. If the distance from the satellite to one of the receivers is significantly less than the distance to the other receiver, the satellite clock bias will not be the same for both receivers. In practice, the satellite bias between the two receivers will be negligible small, but the tropospheric delay will still have influence. The remaining biases after single differencing will be the receiver clock biases, multipath, the integer number of cycles and tropospheric effects.

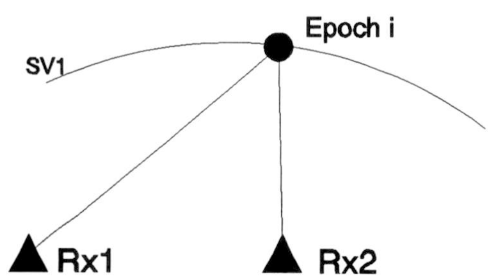

Figure 3-1 Single differences between receivers

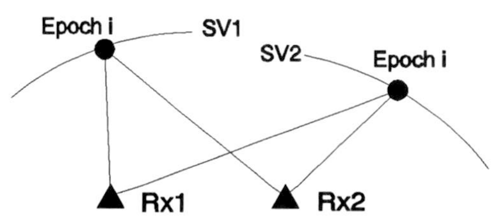

Figure 3-2 Double differences between receivers and satellites

3.3 Double differences

When two receivers track two satellites at the same time, double differences can be taken. Actually, a double difference can be considered to be a difference of two single differences (fig. 3-2). By taking a double difference between receivers and satellites, apart from the biases eliminated during single differencing, the receiver clock bias will be eliminated. The double difference between stations and satellites will therefore in the ideal case not contain any time-dependent biases. In practice, because the two receivers are not located at the same position, position-dependent effects, such as multipath and tropospheric disturbances, will still be present.

After eliminating all satellite biases and time-dependent biases, what is left are the time-independent biases, amongst which the integer number of cycles between the satellites and the receivers, also known as *N-ambiguity*. In some cases, it is possible to determine the value of this (integer number) ambiguity [1]. When the value is known, it does not have to be recomputed during later position calculations, as long as the receiver is able to continuously track the satellite. A known value leaves less unknowns still to be computed, while at the same time it increases the precision of the solution after recomputing, for the number of possible solutions decreases rapidly as soon as some of the ambiguities are fixed.

3.4 Triple differences

In the same way double differences are differences of two single differences, triple differences are differences of two double differences. More precise, a triple difference is the difference of two double differences on two different points in time. (fig. 3-3).

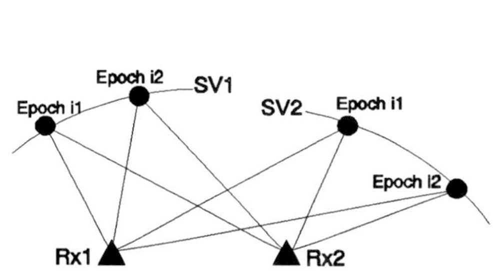

Figure 3-3 Triple difference between receivers, satellites and epochs

Because a double difference contains no time-dependent biases (apart from multipath and tropospheric effects) and the N-bias for a satellite is the same for two different epochs, the triple difference - in the ideal case - will contain no biases at all. In practice, local multipath effects and some tropospheric influences may still be present after triple differencing. Since multipath effects may change as the position of the satellite changes, they may not cancel by triple differencing. When multipath only occurs at only one receiver, from only one satellite and at only one point in time, there is nothing which will cancel this effect. Therefore, multipath may not always cancel entirely.

Since a triple difference is a difference between receivers, satellites *and* epochs, for a given combination of two receivers and two satellites, there is exactly one triple difference. Therefore, it is not necessary to refer to a triple difference between receivers, satellites and epochs, but simply to the triple difference [1].

3.5 The ratio test

The ratio test is a test, developed for determination of the 'true' (or 'most likely') position of a GPS receiver in a grid of possible positions. The grid is formed by the wave fronts of the GPS carrier, as is illustrated in fig. 3-4. In this case, only two wave fronts are drawn, making all the grid points equally likely to be the right position. When a third satellite is used (or when the same satellites are used on a different point of time), extra grid lines will be formed, as shown in fig. 3-5. In a perfect world, exactly one grid point, in the vicinity of the estimated position, would exist where three (or more) grid lines would coincide. This point would be the true position.

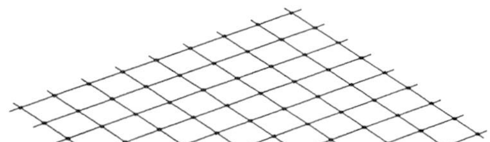

Figure 3-4 Grid of possible positions formed by two satellite carrier waves

Figure 3-5 Grid of possible positions formed by three satellite carrier waves

Unfortunately, in the real world, noise and other disturbances also play a role, so it is not likely that exactly one point can be found where all the wave fronts coincide. Instead of this, the combination of grid lines will produce a number of small areas (the triangles in fig. 3-5), surrounding the possible position solutions (indicated as dots in fig. 3-5). The larger the area, the further away the possible position solution (in the centre of the area) is located from the intersection points of the grid lines, making the position less likely to be the true position.

When a small area, like the encircled area, of fig. 3-5 is magnified, it will look something like fig. 3-6. From this figure, it can be seen that at some of the possible position solutions (marked with a number), the grid lines nearly coincide (5, 8, 9), while at other points the grid lines are much further apart (1, 2, 3, 4, 6, 7).

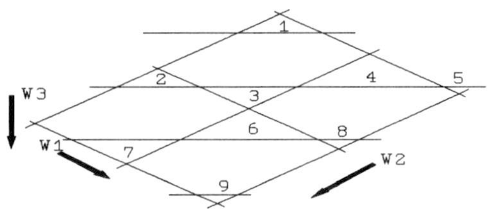

Figure 3-6 Possible position solutions

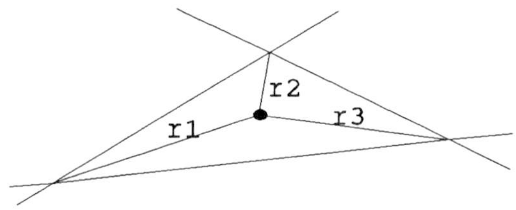

Figure 3-7 Determination of the position residue

To determine at which point the grid lines are closest to each other, a position residue is calculated for each possible position. The way this can be done is illustrated in fig. 3-7. The position solution is considered to be the centre of the triangle. The position residue can be calculated, for example, by taking the sum of the squares of the distances r1, r2 and r3 in the triangle. The larger this sum, the larger the distances r1, r2 and r3 will be (and the larger the area surrounding the possible position solution).

If the residue is small, obviously all the distances from the centre of the triangle to the three vertices are small, so the three grid lines forming the triangle will be very close to each other. The position with the smallest residue will be most likely to be the true position. If, however, two position solutions with (almost) equal residues exist, it will not be possible to decide which one is the true position.

As an indication of the trustworthiness of the position solution found, the ratio between the residue of the second-most likely position and the residue of the most likely position is used. If this ratio is a large number, it means the most likely ('best') position solution is far more likely than the second-most likely ('second-best') position solution, since the area surrounding the latter will be much bigger than the area surrounding the former. If the ratio is a small number, close to unity, the best and second-best position are equally likely, making it impossible to decide which position is the true position.

4 Influence of a dynamical environment on DGPS position solutions

Before the GPS signal can be processed in a computer, it has to be tracked by the GPS card. The carrier wave is tracked using a third-order phaselock loop, the GPS code is tracked using a simple first-order delay lock loop.

Because a third-order phase-locked loop is used for carrier tracking, the filter will be able to track phase accelerations, but will not be able to track a phase jerk [5],[6]. Phase jerk will occur, for example, if the receiver is performing an accelerating turn. During normal flight operation, phase jerk is usually caused by turbulent weather.

A phase jerk will result in a phase error. If this phase error gets too large, the receiver will lose lock. For a receiver, turbulent weather is a worse condition than an accelerating turn, for the phase jerk during turbulence can be considered a phase step, while an accelerating turn will be a phase ramp function. When a phase jerk step function and a phase jerk ramp function are compared, the peak error from the phase jerk step will be 2.43 times larger than the peak error from a comparable phase jerk ramp [5].

During the rotation tests, described in section 5.2.1 and 5.2.2, phase jerk only occurred when the crane or turntable still had to reach the final velocity, or during slowing-down. These periods were very short (less than 2 seconds), so the effect of the phase lag during that period on the calculated position is not visible.

The magnitude of the steady-state error is dependent on the filter bandwidth and the magnitude of the jerk, and can be approximated by [5]:

$$\delta\phi_{ss} = \frac{\Delta\ddot{f}}{\omega_N^{\,3}} = \frac{\Delta\ddot{f}}{(1.2B_L)^3} \qquad (4\text{-}1)$$

where $\delta\phi_{ss}$ is the steady-state phase error, $\Delta\ddot{f}$ the phase jerk (frequency acceleration) and B_L the bandwidth of the filter. As long as the steady-state phase error is less than half a cycle, the receiver will keep a lock on the satellite. During the rotation tests, the small phase jerk present while accelerating or slowing down was much less than half a cycle, so it had no effect on the measurements.

5 Stationary tests, rotation tests and flight tests

When testing the properties of a system, it is desirable to eliminate as many unknown factors as possible before performing the actual test. This chapter will describe the set-up of the tests which have been performed to determine the reliability of the carrier-phase DGPS position solution and the locations where the tests have been done. The test results are presented in chapter 6.

5.1 Stationary measurements: determination of measurement noise

Before starting rotation tests, the amount of measurement noise on the DGPS signal should be known. If there is too much noise, or the test site is such, that only a few satellites are visible at all times, testing doesn't make much sense. This is why a stationary test has been performed.

The test location of the stationary test was the roof of the Electrical Engineering building of the Delft University of Technology. The test antenna was placed approximately 5 meters north-north west of the antenna of the GPS reference station, which is also located on the same roof. Because of the short baseline, it is reasonable to assume that the only difference in signal between the two antennas is caused by noise or multipath.

The test location, with the placement of both GPS antennas, is sketched in fig. 5-1.

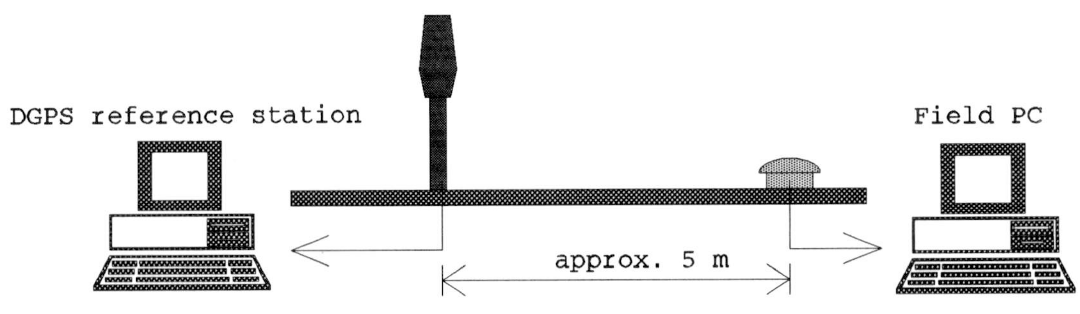

Figure 5-1 Placement of the GPS antennas for stationary noise measurement

5.2 Rotation tests: a controlled dynamical environment

While a stationary test is useful for determining noise and other unwanted signals, it is a very poor approximation of the dynamical properties of an aircraft. A moving antenna is a much better approximation, on condition that the position of the antenna is known during its movement. When the antenna is mounted on a rotating platform, this condition is met, for it is known beforehand that every *t* seconds (where *t* is the rotation time of the platform) the antenna will return to its starting position, thus presenting a means of checking whether the position solution is accurate and reliable.

Another advantage of a rotating platform is its simplicity of construction, making the test equipment itself inexpensive and easy to use.

When a rotating platform is used, it is possible to apply a constant track velocity to the antenna. This is a situation similar to, for example, a curved flight. Due to the rotating motion, the receiver will notice a sinusoidal acceleration towards all satellites in view, with an absolute value dependent of the elevation of the satellites, and a centripetal acceleration towards the centre of rotation. When the acceleration is increased, the receiver will have more difficulty in tracking the signal, possibly resulting in loss of lock or cycle slips due to the limited receiver bandwidth.

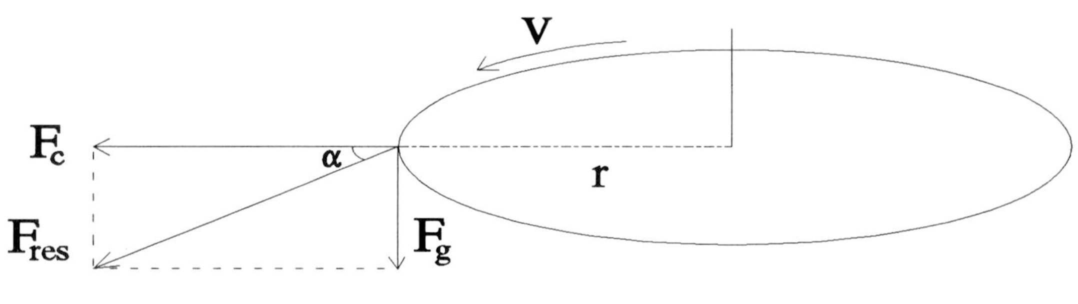

Figure 5-2 Forces applied to a rotating antenna

The idea behind the rotation tests is to apply a controlled acceleration to the antenna which will result in one or more cycle slips without losing lock. When this happens, it will be visible in the position solution as a discontinuity. Since the wavelength of the GPS carrier-phase is 19.05 cm, all possible position solutions are spaced 19.05 cm apart. A cycle slip will thus show as a position leap of approximately 20 cm.

The acceleration of the antenna can be calculated using two well-known physics formulae (see also fig. 5-2):

$$F_c = \frac{mv^2}{r} \tag{5-1}$$

and

$$F = ma \tag{5-2}$$

where

$$v = \frac{2\pi r}{t} \tag{5-3}$$

In the above formulae, F_c is the centripetal force, a is the acceleration, v is the rotating speed, r is the distance from the rotation centre to the antenna and t is the rotation time.

When in formula (5-1) F is substituted by formula (5-2) and v is substituted by formula (5-3), a can be expressed as:

$$a = \frac{4\pi^2 r}{t^2} = 4\pi^2 r f^2 \tag{5-4}$$

where

$$f = \frac{1}{t} \tag{5-5}$$

When the acceleration is too high, the receiver will not function properly anymore because it is working outside its specified acceleration range. This being the case, the result of the ratio test should drop to approximately unity.

5.2.1 A GPS antenna mounted on a harbour crane

During the first rotation test, a GPS antenna was mounted on top of the boom of a small harbour crane, located near the Waalhaven in Rotterdam, approximately 15 kilometres (straight line) from the reference station in Delft. The maximum rotation speed of the crane was 37 seconds, independent of the rotation direction. The radius from the point of rotation to the antenna during the test was 12 meters. During the test, when the crane rotated, it rotated at maximum speed. The acceleration at the antenna, according to formula (5-4), was only 0.346 m/s², or 0.0353*g*, where *g* is the acceleration of gravity.

Unfortunately, probably due to the environment, during the test only three satellites were locked continuously by the GPS receiver, although eight to ten satellites were visible. The three satellites continuously in lock were all located in the west, which is a good reason to believe that the test site in the Waalhaven was not very 'GPS-friendly'. A picture of the test location and a schematic sketch of the test location and its environment can be found in appendix 1.

The test data was gathered according to the following scheme:

	Duration
Initialization of the receiver; two 90° turns clockwise	13 min.
Rotation clockwise at maximum rotation speed (10°/s)	5 min.
Stationary measurements	2 min.
Rotation counter-clockwise at maximum rotation speed (10°/s)	5 min.
Stationary measurements	1 min.

Table 5-1 Measurement scheme during crane test

The two 90° turns during initialization were an attempt to find a place where more than three satellites would be in continuous lock. As already stated, the attempt failed. The 2 minutes stationary measurements between the clockwise and counter-clockwise rotation were inserted as a recognition mark between the two opposite rotation directions. The rotation direction was taken both clockwise and counter-clockwise to check whether the direction of rotation has any influence on the quality of the received signal. As could be expected, this was not the case. Therefore, the direction of rotation during the turntable test (section 5.2.2) was only taken clockwise.

5.2.2 A GPS antenna mounted on a turntable (first test)

To be able to perform rotation tests in a somewhat less 'GPS-unfriendly' environment than the Waalhaven, a small turntable has been constructed. This turntable consists of a linear DC motor driving a platform. On this platform, two aluminium bars (each with a length of two meters) are mounted. A GPS antenna is attached to one of them. In the centre of the platform, a portable, battery-powered, computer is mounted. The antenna and computer are connected via a small antenna cable. Some guy ropes are used to prevent the aluminium bars from bending or vibrating too much. A picture of the turntable and a sketch with the dimensions can be found in appendix 2.

With the equipment described, a rotation test has been performed on the roof of the Electrical Engineering building of the Delft University of Technology. The turntable was located approximately 5 meters from the GPS reference station antenna. Data measurements have been done with different rotation frequencies, as indicated in table 5-2. The acceleration is calculated using the second part of formula (5-4).

	Frequency	Duration	Acceleration
Clockwise rotation	0.47 Hz	4' 10"	15.05 m/s² ≙ 1.54g
Stationary measurement	-	0' 18"	-
Clockwise rotation	0.73 Hz	5' 08"	36.32 m/s² ≙ 3.70g
Stationary measurement	-	0' 42"	-
Clockwise rotation	0.97 Hz	5' 25"	64.12 m/s² ≙ 6.54g

Table 5-2 Measurement scheme during first turntable test

As can be seen from the table, at 0.97 Hz the acceleration is over 6g. Since the used GPS receiver can only deal with accelerations smaller than 4g [4], it can be predicted that the GPS receiver will not be able to function correctly under these conditions. As will be shown from the results in chapter 6 and the Geotracer output file in appendix 5, the value of the ratio test during this interval will drop to approximately unity.

5.2.3 A GPS antenna mounted on a turntable (second test)

A test similar to the turntable test described in section 5.2.2 has been performed using a slightly different set-up. The main differences between this second turntable test and the first one are the location of the reference antenna and the placement of the turntable itself. To investigate the height variation found during the first turntable test, the entire turntable was rotated 90° to check whether the height variation was caused by the environment or by the turntable itself.

The reference antenna was placed approximately 500 metres from the Electrical Engineering building on a hockey-field, to investigate whether the distance between the reference antenna and the rotating antenna would affect the value of the ratio test. Unfortunately, because of an error in the software used to gather the GPS data, not the entire dataset from this reference antenna was useable. It was not even possible to calculate its exact position, so in fact the antenna was of little use.

Because of the problems with the software, the position of the rotating antenna during this rotation test was also calculated by using the reference antenna on the roof of the Electrical Engineering building. The measurement scheme during this test was:

	Frequency	Duration	Acceleration
Clockwise rotation	0.47 Hz	3' 00"	15.05 m/s² ≙ 1.54*g*
Stationary measurement	-	0' 20"	-
Clockwise rotation	0.73 Hz	3' 00"	36.32 m/s² ≙ 3.70*g*
Stationary measurement	-	0' 20"	-
Clockwise rotation	0.97 Hz	3' 00"	64.12 m/s² ≙ 6.54*g*
Clockwise rotation	0.90 Hz	0' 30"	55.00 m/s² ≙ 5.61*g*
Clockwise rotation	0.82 Hz	0' 30'	45.66 m/s² ≙ 4.65*g*
Clockwise rotation	0.78 Hz	0' 30"	41.31 m/s² ≙ 4.21*g*

Table 5-3 Measurement scheme during the second turntable test

The last three measurements (0.90 to 0.78 Hz) were used to investigate the behaviour of the GPS card after loss of lock, which occurred during the 0.97 Hz data interval. The results of the test can be found in chapter 6.

5.3 Flight tests: an uncontrolled dynamical environment

Although the rotation tests are a reasonable approximation of flying, they are still restricted to only one position and only a horizontal plane. In order to find out whether the behaviour of carrier-phase DGPS position solutions is 'better' under controlled conditions than in reality, test data from real flight tests was also processed for comparison.

The difficulty with real flight test data is the uncertainty about the true position. During the stationary test, the location of the receiver was known up to a few centimetres. During the rotation tests, the uncertainty increased a little, but still it was possible to validate the position solutions by comparing the positions found during one revolution to the positions found during another. Flight tests do not provide such a validation possibility. The only way to validate the position solutions is to split the measured data in overlapping parts, process the parts separately and compare the position solutions from one part to the corresponding position solution of the other, overlapping, part. When the position solution of both overlapping parts is the same, the position solution found can be believed to be the right one.

6 Post-processing software and test results

Raw carrier-phase GPS data are post-processed to obtain a position solution. The software used for the calculation of the carrier-phase DGPS position solution is called 'Geotracer'. This program is normally used for post-processing flight data to provide a truth reference. All of the test data and flight test data were processed using the Geotracer software.

This chapter will start with a short description of the Geotracer software. After that, the results of the different tests will be presented and, when necessary, discussed.

6.1 The Geotracer software

The Geotracer software is capable of post-processing raw GPS data in various ways. It can be used to calculate distances between stationary receivers (GPS or DGPS position solutions) or to calculate the position of a (not necessarily stationary) receiver with respect to a stationary reference station ('Static' positioning for a stationary receiver and 'On the fly' positioning for a moving receiver). In the latter cases, carrier-phase DGPS is used for accurate positioning. Since most of the tests were performed using a moving receiver, all of the test data have been processed using the 'on the fly' mode of Geotracer. The stationary data was processed in both 'on the fly' and 'static' mode to determine the effects of noise and multipath on the position solution.

The antenna of the reference station used during the stationary and rotation tests was located on the roof of the Electrical Engineering building of the Delft University of Technology. The antenna of the reference station used during the flight tests was located at Boscombe Down airport in the United Kingdom [3].

Before processing carrier-phase DGPS data, an estimated position for both reference station and moving receiver is calculated, based on the GPS code measurements. The coordinates of the reference station are then set fixed, in order to have a stationary reference. When this has been done, the carrier-phase DGPS position of the moving receiver can be calculated by taking single, double and triple differences, in the way which is described in chapter 3.

The Geotracer program uses the ratio test to decide whether to accept a calculated position or to reject it. By default, a ratio smaller than or equal to 2 will reject the calculated position, while a value larger than 2 will result in acceptance of the calculated position. Why the acceptance threshold is set to 2 is not clear. For geodetic applications, a much lower value of 1.3 is used [8], while the rotation test data and the flight test data showed that the calculated position solution could be wrong even when the value of the ratio test was larger than 2.

6.2 Stationary test results

By processing stationary data 'on the fly', multipath effects and receiver noise will become visible. Since the antenna was stationary (at least with respect to the antenna of the reference station), the observed 'movement' of the antenna will be a measure of the noise of the receiver and multipath effects under a changing satellite configuration.

Multipath effects in a stationary receiver are caused by satellite movement, as shown in fig. 6-1.

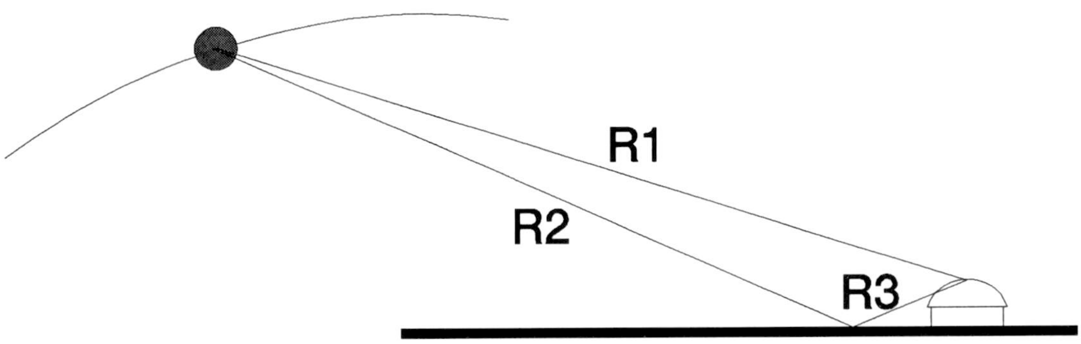

Figure 6-1 Multipath signals at a stationary receiver

When $R2 + R3 = R1 + k\lambda$ $(k = 1,2,3,...)$, where λ is the wavelength of the GPS carrier signal, the reflected signal will constructively interfere with the direct signal. If, on the other hand, $R2 + R3 = R1 + \frac{2k-1}{2}\lambda$ $(k = 1,2,3...)$, the reflected signal will destructively interfere with the direct signal. In between those two extremes, the signal strength at the receiver will slowly increase or decrease. Because the satellites are in continuous motion, the distances R1, R2 and R3 are also continuously changing. The effect of this will be a sinusoidal change in signal strength at the receiver.

The position solution after post processing did indeed show some noise and multipath effects. This can be seen in fig. 6-2a - 6-2c, especially in fig 6-2b. These three figures represent the variations in longitude, latitude and height, respectively, against time.

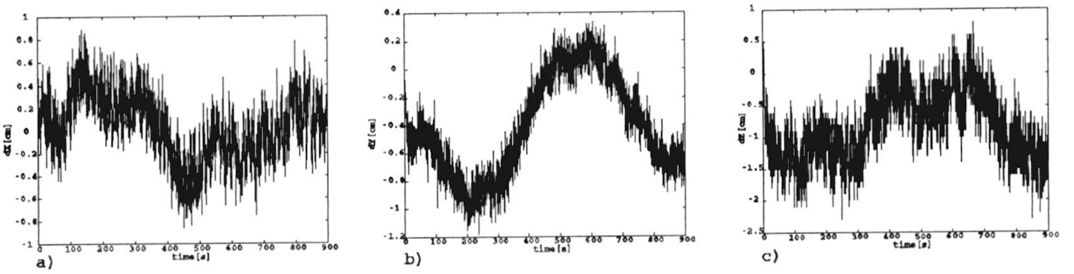

Figure 6-2 Position deviations of the stationary antenna due to noise and multipath effects a) longitude vs. time b) latitude vs. time c) height vs. time

The full-size pictures are included in appendix 3. The pictures on this page are only included as a quick reference.

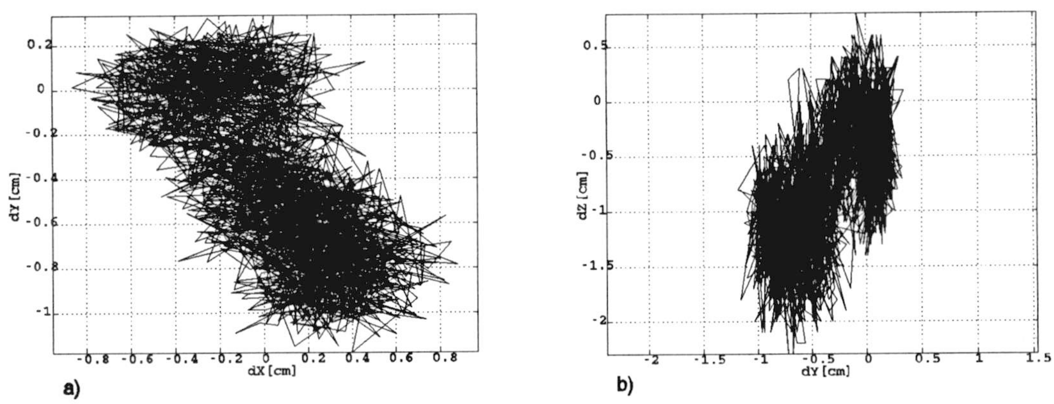

Figure 6-3 Position deviations of a stationary receiver. a) longitude vs. latitude b) latitude vs. height

When the position deviation in latitude is plotted against the position deviation in longitude, the plot does not show a circle, as might be expected, but a slightly tilted ellipse (fig. 6-3a). This effect might be explained by the satellite configuration, or in this case, by the number of satellites, since the test receiver had only 5 satellites in lock. Four of them were located east or west of the antenna, thus providing a much better correction in the east-west direction than in the north-south direction.

The plot of the deviation in latitude against the deviation in height (fig 6-3b) shows another remarkable phenomenon: a latitude-dependent height offset. This, however, can be explained by simple geometry: If the (absolute) distance between two objects is constant and the horizontal distance increases (because of the noise in the latitude direction), the vertical distance has to decrease, according to the Pythagorean theorem. So whenever the receiver noise caused a position shift in latitude, the height would change also.

6.3 Test results with a rotating antenna

As mentioned in chapter 5, the first rotation test was performed with a GPS antenna mounted on top of the boom of a small crane. Since the rotation speed of the crane was not very high, no cycle slips were to be expected. Unfortunately, only three satellites were tracked continuously. The other visible satellites were locked, but were marked 'bad health' or 'misclosure too large'. The reason why this happened is still unknown. It does indicate, however, that GPS is still not guaranteed to work everywhere.

After post-processing the GPS data, it turned out that the carrier-phase positioning had not suffered very much from the tracking problems. According to the Geotracer software, the carrier-phase position solution was based on six or seven satellites. In spite of this, the position solution was not a perfect circle. In the north-south direction, the various position solutions were as much as 25 cm (more than a wavelength) apart. In the east-West direction, the position solutions were much closer, as can be seen in fig. 6-4. The same effect can be seen in the code position solution (fig 6-5).

The disturbances that can be seen in the upper part of this figure may very well be multipath effects, caused by reflections of the signal against the mast and derricks (see fig A1-2). The broadening of the graphs in the north-south direction can be explained by the satellite configuration; because the east-west geometry is often better than the north-south geometry, the positioning accuracy in east-west direction will be better than in the north-south direction.

Both position plots are included full-size in appendix 4.

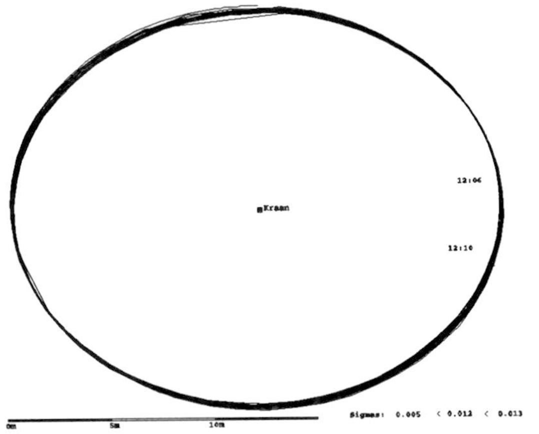

Figure 6-4 Carrier phase DGPS position solution of the Waalhaven test.

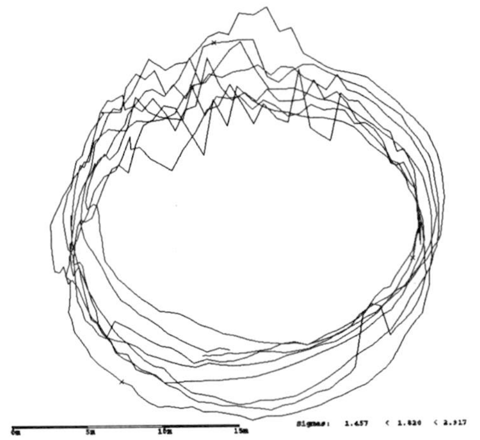

Figure 6-5 Code position solution of the Waalhaven test

The position solution of the turntable tests was quite a lot better than the position solution of the Waalhaven test. There are two main reasons for this. The first reason is the (much shorter) distance between the moving antenna and the reference antenna. While during the Waalhaven tests the baseline was approximately 15 km, the mean baseline during the turntable tests was only 5 metres. The influence of tropospheric effects could thus safely be neglected during the turntable test. The second reason for better results during the turntable test is also position-dependent. During the Waalhaven test, only 3 satellites could be tracked continuously, while 5 other satellites were tracked intermittently. The test site caused a lot of interference and reflections because of the environment. During the turntable test, 7 or 8 satellites were tracked continuously, while the antenna was not shielded from the satellite signals by trees or high objects, because the test location was on top of one of the highest buildings of Delft.

The position solution of the turntable test does indeed show an almost perfect circle (fig 6-6). At a closer view, it will in fact show 2 circles very close together. The second circle is the result of a position solution during a part of the test where the receiver was working well beyond its specifications (6g). This caused the value of the ratio test to drop dramatically, from a value of over 78 (initial value) when working within its specified range to a value of only 1.06 when working beyond its specifications (see appendix 5 for the Geotracer output file). If this part of the data is deleted, the position solution will be a perfect circle (fig 6-7). Both of the figures can be found full-size in appendix 4.

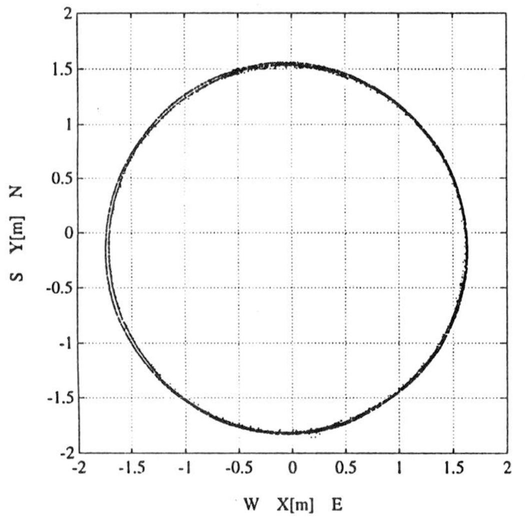

Figure 6-6 position solution of the turn-table test

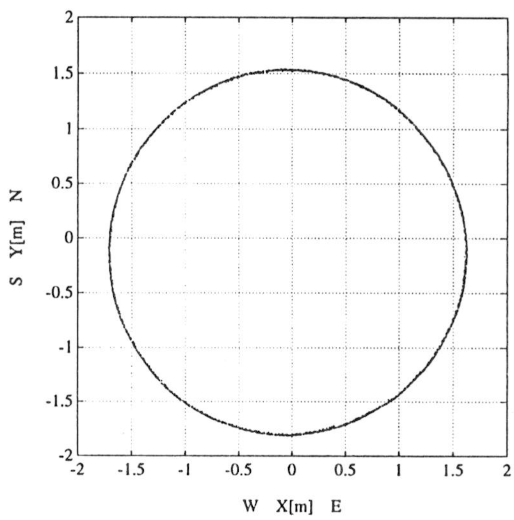

Figure 6-7 Position solution of the turn-table test (receiver working within specifications)

When the height is considered, a periodic variation can be seen. This variation was visible during the entire test, so it is likely that it is caused by the location of the test equipment or the test equipment itself. The variation in height is made visible in fig. 6-8 (receiver working within specifications) and fig. 6-9 (receiver working beyond its specified acceleration range). The lower part of both plots is the variation in height, which, as can be seen, is approximately 8 cm peak to peak.

The direction of rotation during the test was clockwise, so from the X- and Y-signals (upper part of both plots), it can be seen that the variation in height occurred in exactly south-west direction. It is not likely that multipath caused the variation, since the variation seems to be a stationary effect (visible in the same direction during the entire duration of the test). The variation is not caused by a tilt angle of the turntable either, since in that case the variation would have been sinusoidal. The turntable itself has been checked for irregularities, but nothing obvious has been found that could have caused a 6 cm periodic variation. The only thing left that may have caused the height variation is a variation in rotating speed, which may be caused by a slight irregularity in the driving belt or the driving wheels of the turntable.

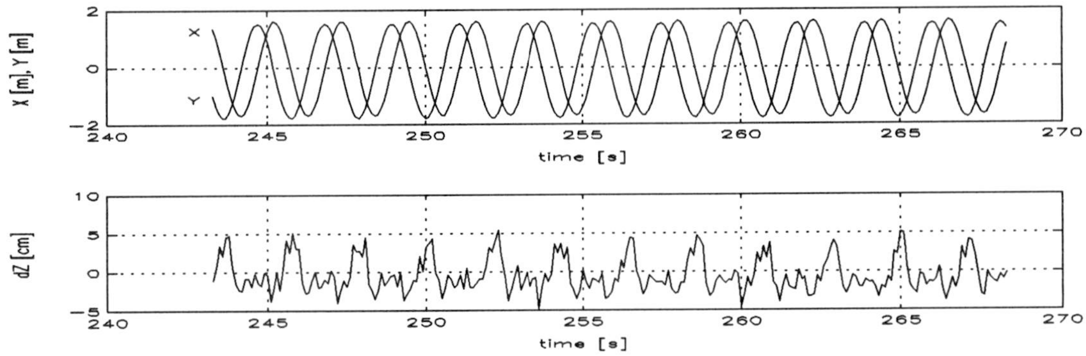

Figure 6-8 Turntable position solution vs. time (receiver operating within specifications)

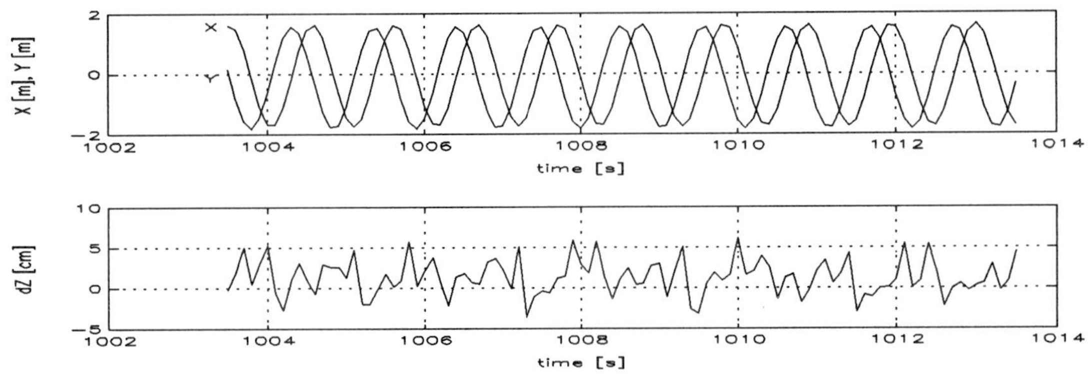

Figure 6-9 Turntable position solution vs. time (receiver operating beyond specified acceleration range)

If the variation is caused by an irregularity in the test equipment, a similar variation should be visible in the horizontal plane. As can be seen in figure 6-10, this is indeed the case (upper plot: height variation, lower plot: variation in distance from the antenna to the center of rotation). The center of rotation (at coordinates (X_0,Y_0)), is calculated by taking the point midway of the minimum and maximum X- and Y- coordinates. The distance D to that point is calculated by:

$$D=\sqrt{(X-X_0)^2+(Y-Y_0)^2} \tag{6-1}$$

In formula (6-1), X_0 and Y_0 are the coordinates of the centre of rotation and X and Y are coordinates on a circle with radius *D* to the centre of rotation. Since the radius was constant during the tests, every variation of the radius will be the result of external influences.

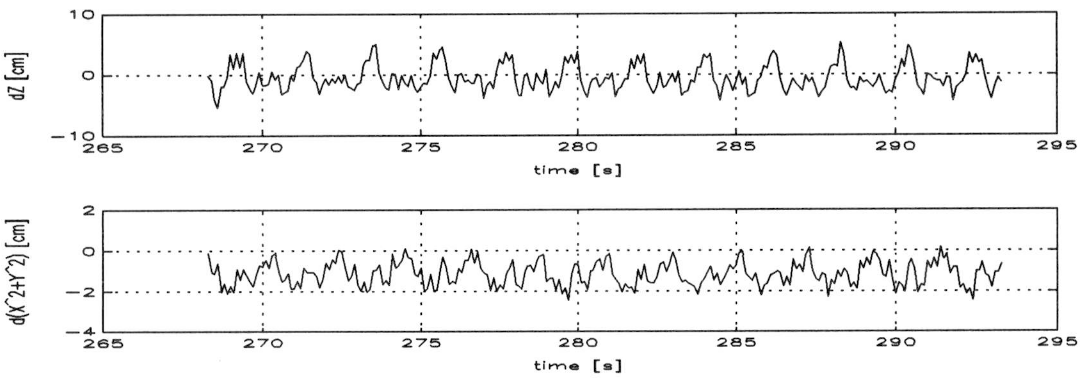

Figure 6-10 *Variation in height and variation in distance to the centre of rotation during the turntable test*

As can be seen from the figure (6-10), the variation in height and the variation in distance to the centre of rotation are 180° out of phase, as might be expected, since the total distance did not change. A positive variation in height will thus mean a negative variation in distance and vice versa.

Since a periodic variation (whose frequency depends on the rotating frequency of the turntable) is visible in both height and distance, it is safe to conclude that this variation is caused by the test equipment itself, and not by the environment. This assumption seems to be confirmed by the second turntable test, during which the turntable was located on the same position as during the first turntable test, but rotated 90° counter-clockwise entirely. As can be seen from figure 6-11, the height variation has been moved to another position, from due south-west to due south-east, 90° counter-clockwise from its original position, as was expected.

The second turntable test also proved that cycle slips are possible even when the value of the ratio test is much larger than 2. As can be seen in the Geotracer output file in appendix 6, the ambiguities to satellites 7 and 29 are calculated twice, resulting in two different ambiguity values. Both of the calculations, however, returned a ratio test value larger than 4. It is therefore proven that a large ratio value is no guarantee for a good position solution.

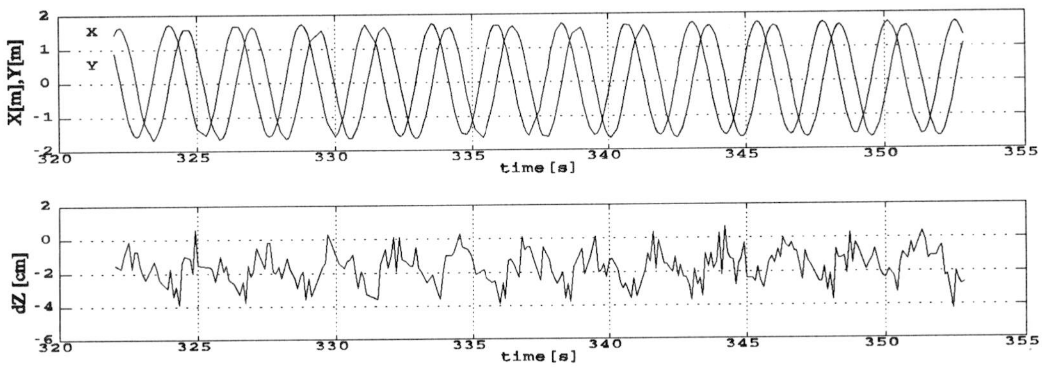

Figure 6-11 Turntable position solution vs. time (second turntable test)

6.4 Comparison of the test results to the results of a flight test

The test results from the turntable test and the crane test have been compared to flight test data. It turned out that the effects of a small ratio value during all the tests did not necessarily mean that the position solution was incorrect. When the right ambiguities had already been fixed during a period with a large ratio value, a ratio value much smaller than the threshold value of 2 also provided the right position solutions (within margins). An example can be found in appendix 5 and section 6.3, fig. 6-6 and 6-7. As can be seen from appendix 5, the already found ambiguities from the turntable test did not change when they were recomputed during the 0.97 Hz data. This is caused partly by the way the Geotracer program handles ambiguities when the ratio test returns a small value. If the ratio test returns a small value, the Geotracer program just holds the already known ambiguity values. From fig 6-6, it can be seen that the position solution from the 0.97 Hz rotation data returns a 'false' position. The difference between this 'false' position and the 'true' position is, however, only 7 centimetres. This is calculated by taking the difference between the minimum and maximum values of the X- and Y- data from the part of the data where the receiver was working within specifications and the minimum and maximum values of the X- and Y- data from the part of the data where the receiver was working beyond its specified area. The maximum difference observed turned out to be only 7 centimetres.

On the other hand, when the initial ambiguities were fixed with a ratio value slightly larger than the threshold value, the ratio test afterwards returned very large values, in spite of the fact that the ambiguities were not fixed correctly. The 'right' values of the ambiguities in this case were already computed from a part of the data which returned an initial ratio value larger than 6 or 7. It is not stated that those values were correct, but the ambiguities found in the latter case (ratio 6 or 7) do have a higher probability of being the right ones. Since the ratio test returns the ratio of the standard deviation of the best position solution and the standard deviation of the second-best position solution, if the value of this ratio is high, either the best solution has a very small standard deviation or the second-best solution has a much larger standard deviation than the best solution. In both cases, the best position solution is much more likely than the second-best position solution.

An example of a Geotracer output file, showing the fact that a high value for the ratio test does not necessarily mean the right ambiguities have been fixed, can be found in appendix 6. The set-up of the turntable test, to which this output file belongs, was such that the GPS receiver was guaranteed to lose its position for three minutes without losing its lock on the satellites. After those three minutes, the rotating speed was decreased to an acceptable value (from the receiver point of view) and the receiver was able to fix its position again and to recompute the ambiguities to the satellites in view. It turned out that some of the ambiguities fixed after losing position lock were different from the ambiguities fixed to the same satellites before position lock, in spite of a ratio value larger than 4 in both cases.

7 Conclusions and recommendations

7.1 Conclusions

When post-processing carrier-phase DGPS data, the ratio test is used as a quality indicator for the calculated position solutions. Intuitively, the larger the value of the ratio test, the better the position solution will be. This, however, is not always true. Once a wrong position solution is accepted because it just satisfied the test conditions (a value slightly larger than a set threshold), the positions that are calculated afterwards may return ratio values of well over 100 because the already found ambiguities are held fixed. Still, the position solution is not true.

The value of the threshold is a question still unanswered. The threshold used in Geotracer (ratio > 2) and the value used for geodetic applications (ratio > 1.3) seem to be empirical values with an accepted error-probability. However, since the probability distribution of the ratio is unknown, it is not clear what the accepted error-probability will be. The turntable tests have shown that both values are too low for a reliable position solution, but an absolute value for the threshold can still not be given.

The conclusions of the research, described in this report, are:

1. The ratio test can be used as a rough quality indicator for the calculated carrier-phase DGPS position solutions, in so far that a larger value of the ratio test indicates a higher probability of having found the right ambiguities. However, the ratio test is not capable of indicating whether the calculated position is the true position.
2. When using the ratio test as a quality indicator, care should be taken not to trust the calculated position solution blindly. Especially when the first ambiguity fix resulted in a low value of the ratio test or the position fix was lost and recovered again, later values of the ratio test may be large while the calculated position may still be wrong.

7.2 Recommendations

To prevent the ratio test from returning a large value when initially the wrong ambiguities were fixed, every time a new ambiguity is computed (for example, when a new satellite becomes visible), the other ambiguities should be recomputed. This, however, will result in longer computing times and a less accurate position solution when the initial ambiguities were the right ones. It is therefore not a very practical solution.

When absolute certainty about the correctness of the position solution is necessary, the raw GPS data should be processed in different, partly overlapping parts. When all the overlapping parts of the final position solution agree, chances are that it is the right position solution.

References

[1] Brouwer, F.J.J et al, *Navigatie en geodetische puntsbepaling met het global positioning system*. Delft, 1992. Delft University of Technology, Faculty of Geodetic Engineering. Lecture notes on a GPS-course.

[2] Forssell, B, *Radionavigation systems*. Prentice-Hall, 1991.

[3] Goor, S.P. van and M.B. Zaaijer, *Set-up of a DGPS airborne system using the MLS data broadcast in DRA's BAC 1-11*, Delft, 1996. Delft University of Technology, Faculty of Electrical Engineering. Contract report.

[4] NovAtel, *GPSCArd user manual*. NovAtel Communications Inc., 1993.

[5] Parkinson, Bradford W and James J. Spilker Jr [ed], *Global Positioning System: Theory and Applications Volume 1*. American Institute of Aeronautics and Astronautics Inc., 1996.

[6] Spilker, James J Jr, *Digital Communications by Satellite*. Prentice-Hall, 1977.

[7] Willigen, D. van, *Radio plaatsbepaling*. Delft, 1995. Delft University of Technology, Faculty of Electrical Engineering. Lecture notes on et03-31.

[8] Zand, R.J. van 't, *Validatie van de LAMBDA-methode - Een onderzoek naar de prestaties van een nieuwe methode voor het schatten van meerduidigheden en de bruikbaarheid van validatietoetsen*. Delft, 1994. Delft University of Technology, Faculty of Geodetic Engineering. Thesis report.

Appendices

Appendix 1 The Waalhaven test location

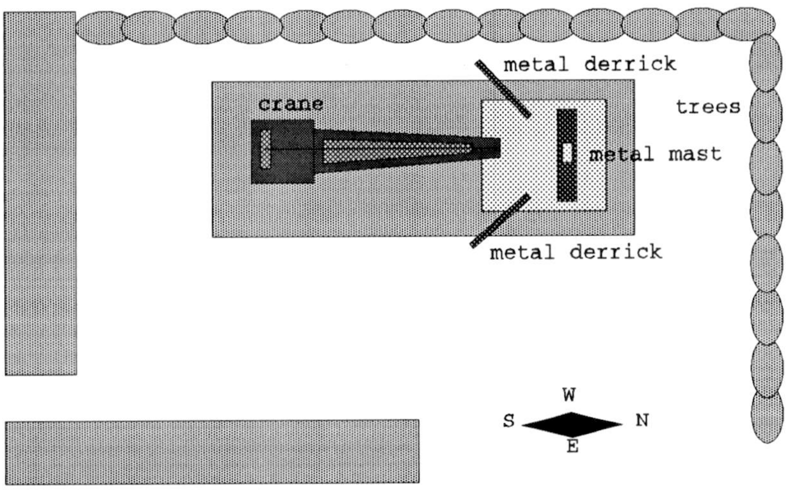

Figure A1-1 *The Waalhaven test location (overview)*

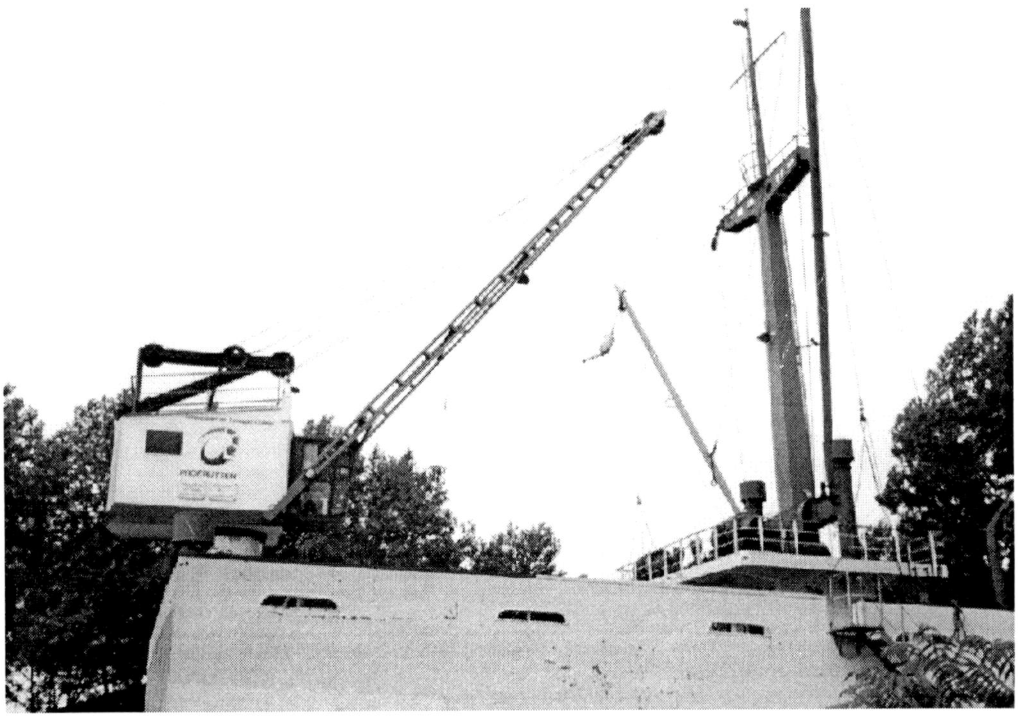

Figure A1-2 *The Waalhaven test location*

As can be seen in fig. A1-1, the Waalhaven test location was surrounded by trees in the north and west, and by buildings in the south and east. The crane, on which the antenna was mounted, is rigidly fixed to the middle part of an old ship (fig A1-2). This ensures an almost vibrationless rotation of the crane.

In the north, a metal mast and two metal derricks are mounted on the ship, blocking the GPS signals coming from the north and reflecting all signals from the southern directions The GPS antenna was mounted on top of the boom of the crane, which was raised higher than the roofs of the surrounding buildings and almost as high as the surrounding trees.

Appendix 2 The Delft University of Technology turntable

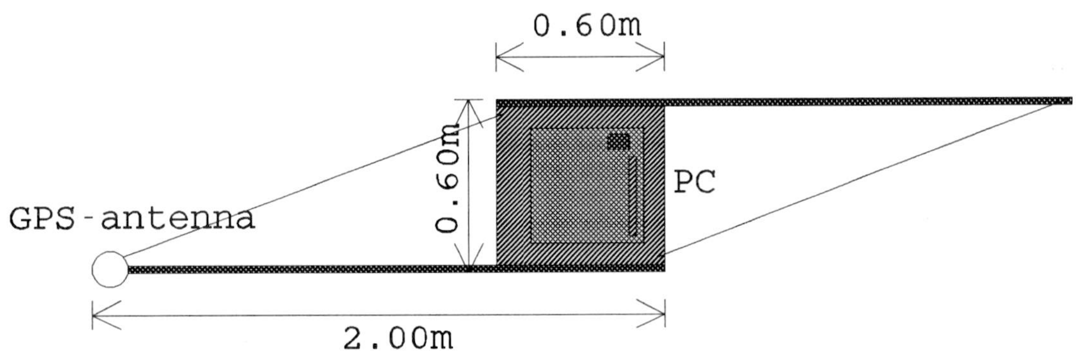

Figure A2-1 Sketch of the Delft University of Technology turntable

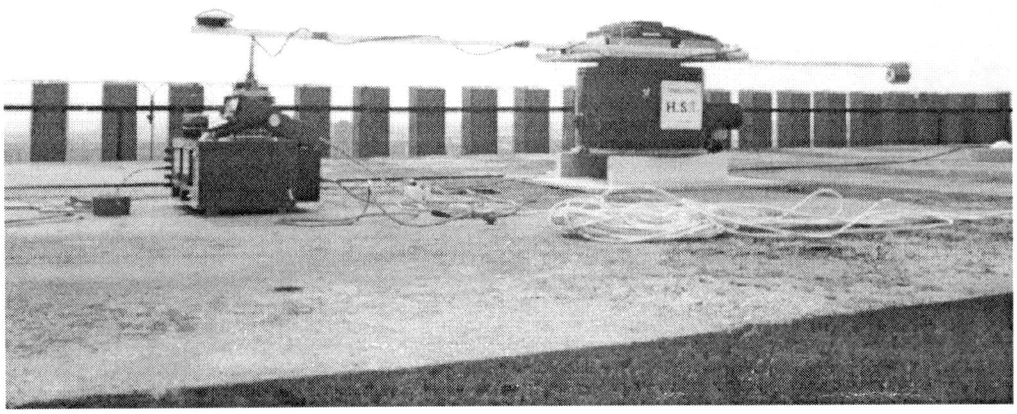

Figure A2-2 The Delft University of Technology turntable during the tests

The turntable used during the rotation tests consists of the drum of a washing machine (inner and outer drum and the motor), fixed rigidly to a wooden under-carriage, and a wooden platform, 60 x 60 centimetres, fixed to the inner drum of the washing machine, on which two aluminium tubes were mounted. At the end of one of the tubes, a GPS antenna was mounted. On the platform, room was left for a portable PC, which was used to gather the GPS data.

The motor of the washing machine was powered by a stabilized, adjustable power supply, which was used to control the rotating-speed of the platform.

Appendix 3 Noise and multipath effects at a stationary receiver

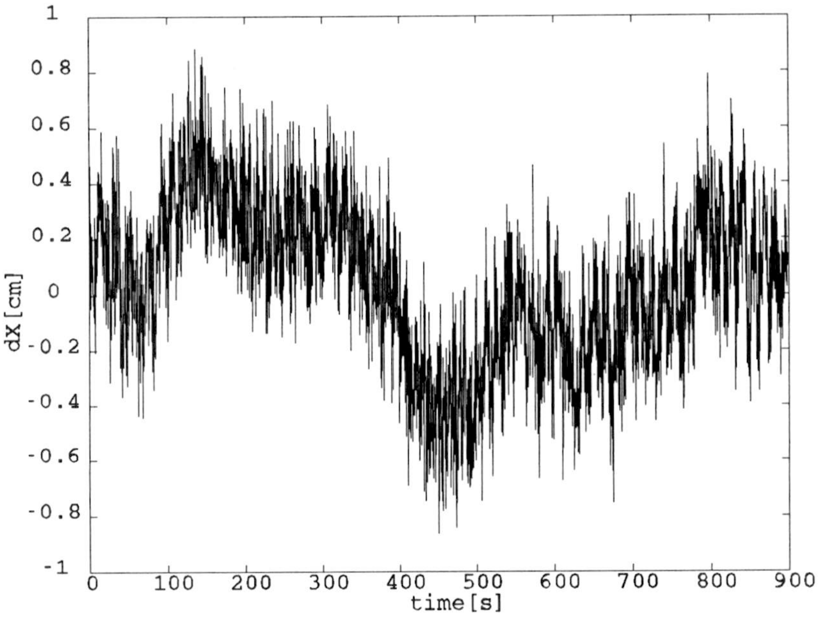

Figure A3-1 *Deviation in longitude caused by receiver noise and multipath*

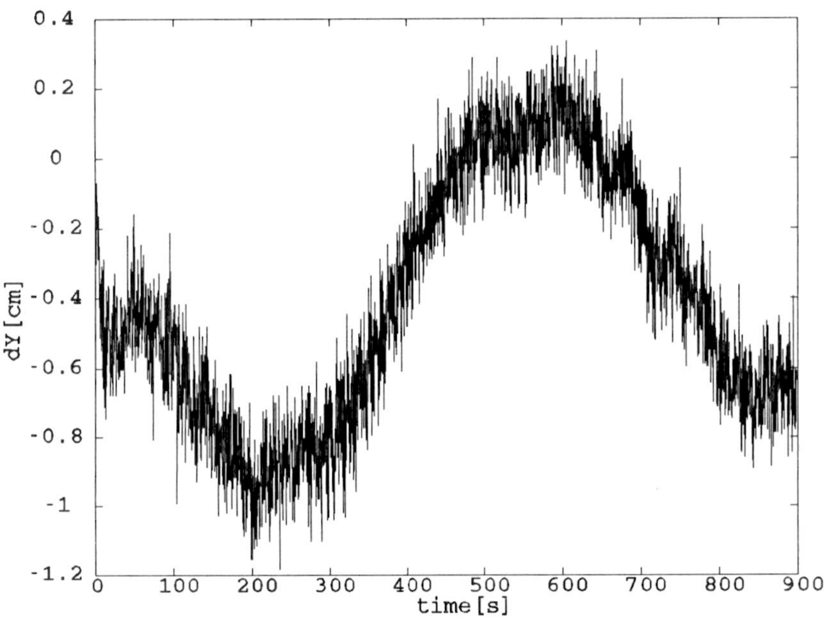

Figure A3-2 *Deviation in latitude caused by receiver noise and multipath*

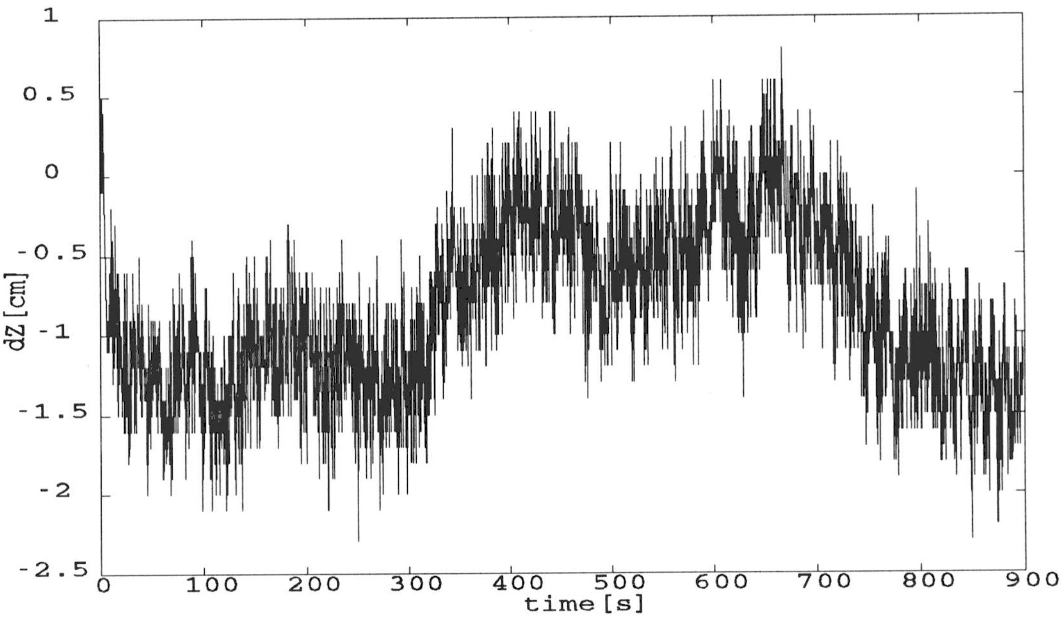

Figure A3-3 *Deviation in height caused by receiver noise and multipath*

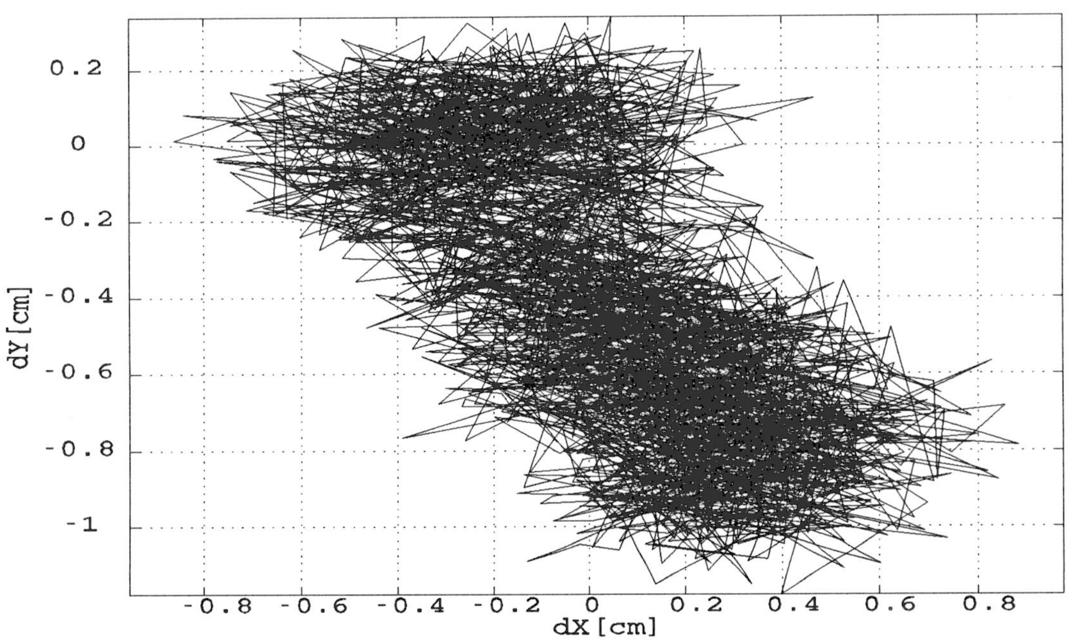

Figure A3-4 *Latitude deviation vs. longitude deviation*

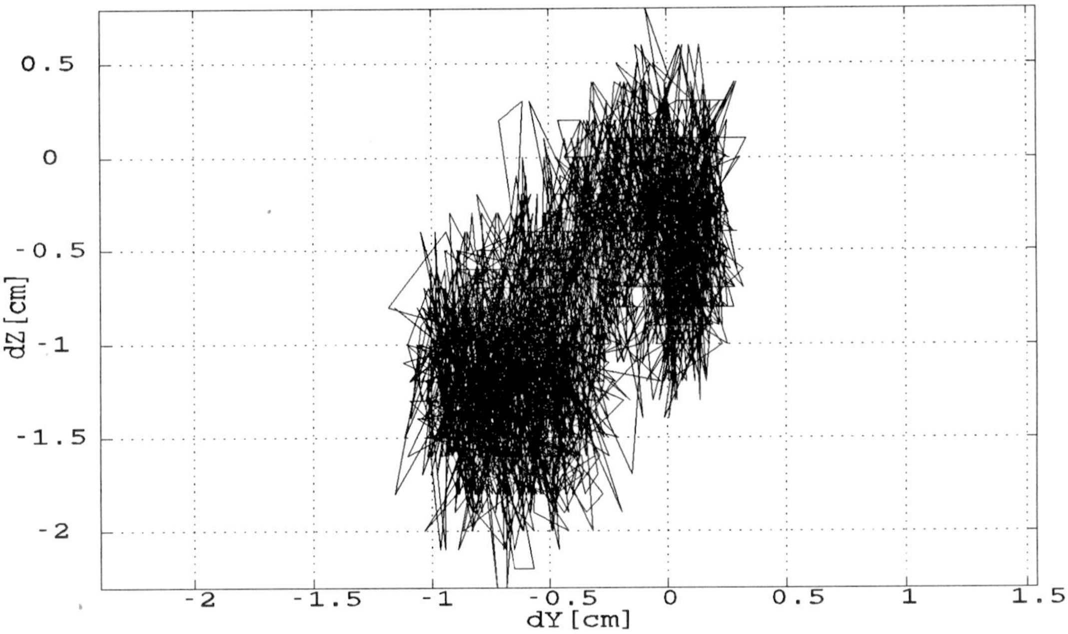

Figure A3-5 *Latitude deviation vs. height deviation*

Appendix 4 Position plots of the rotation tests

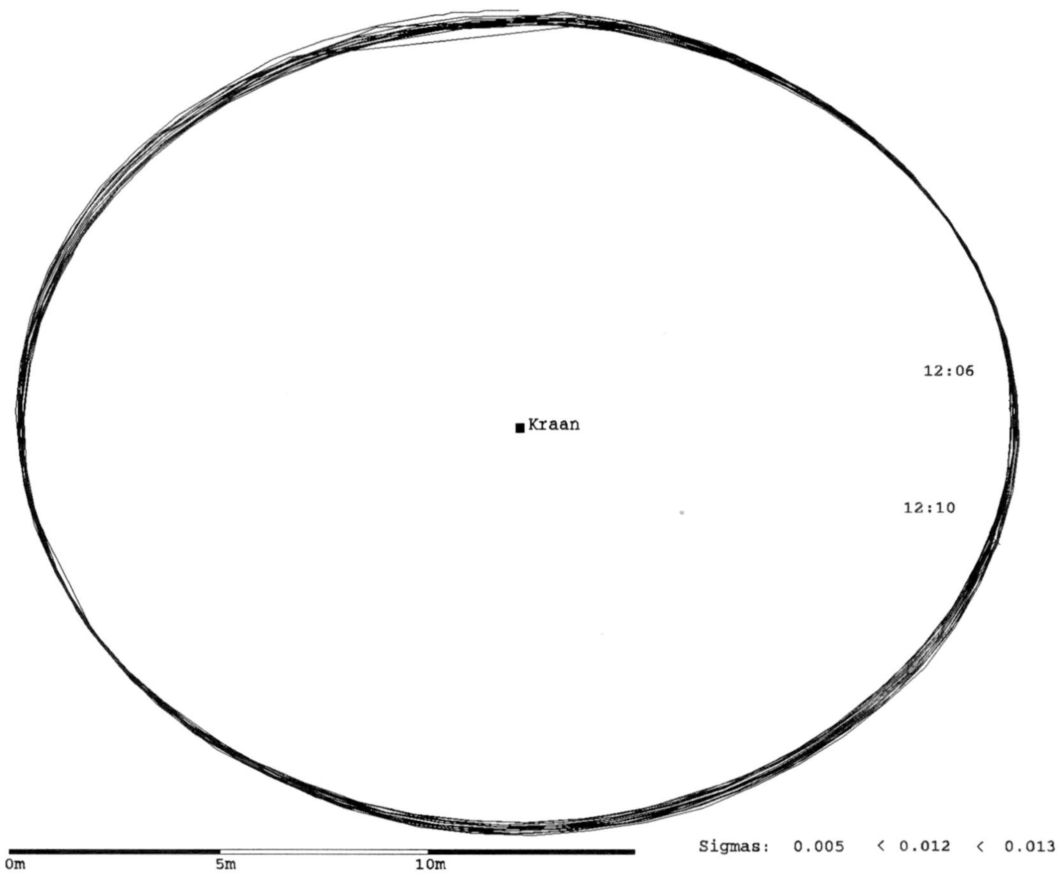

Figure A4-1 *Carrier phase DGPS position solution of the Waalhaven test (counter-clockwise rotation)*

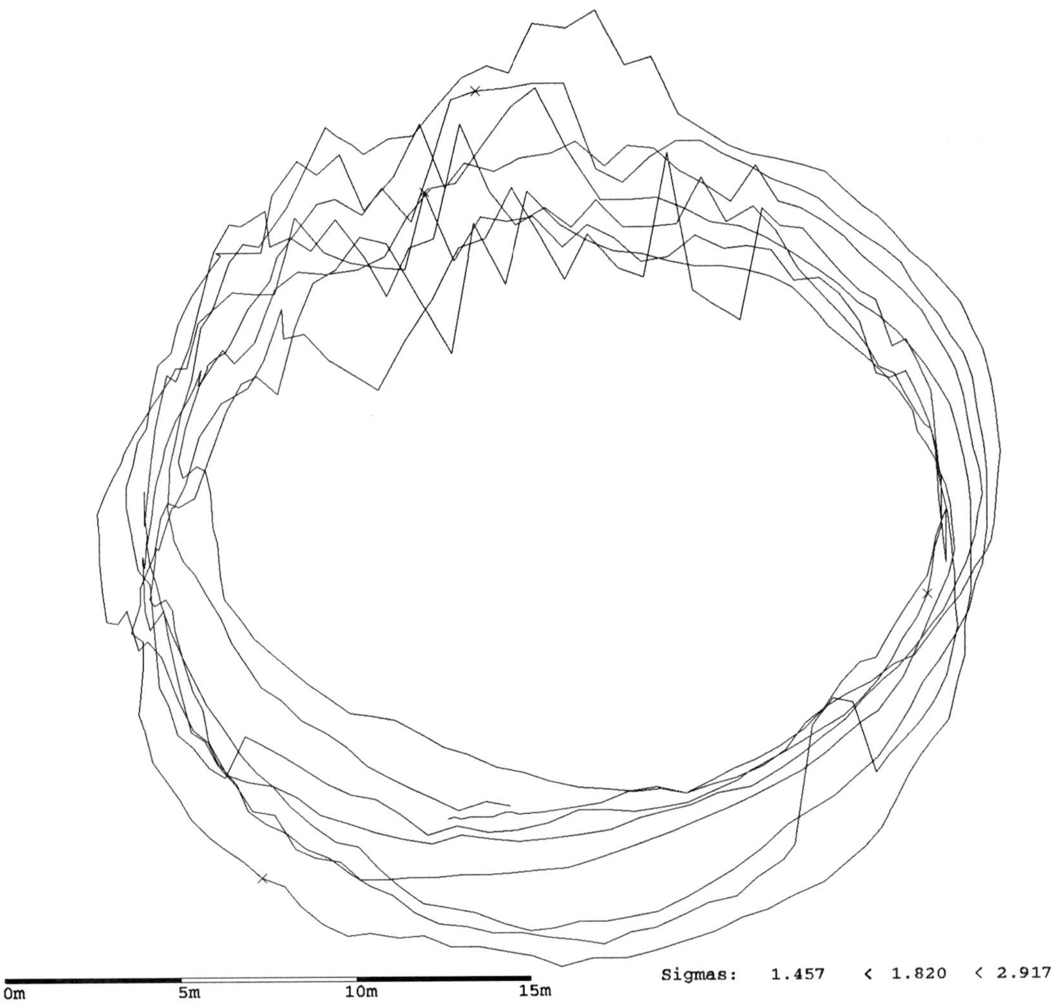

Figure A4-2 *Code position solution of the Waalhaven test (counter-clockwise rotation)*

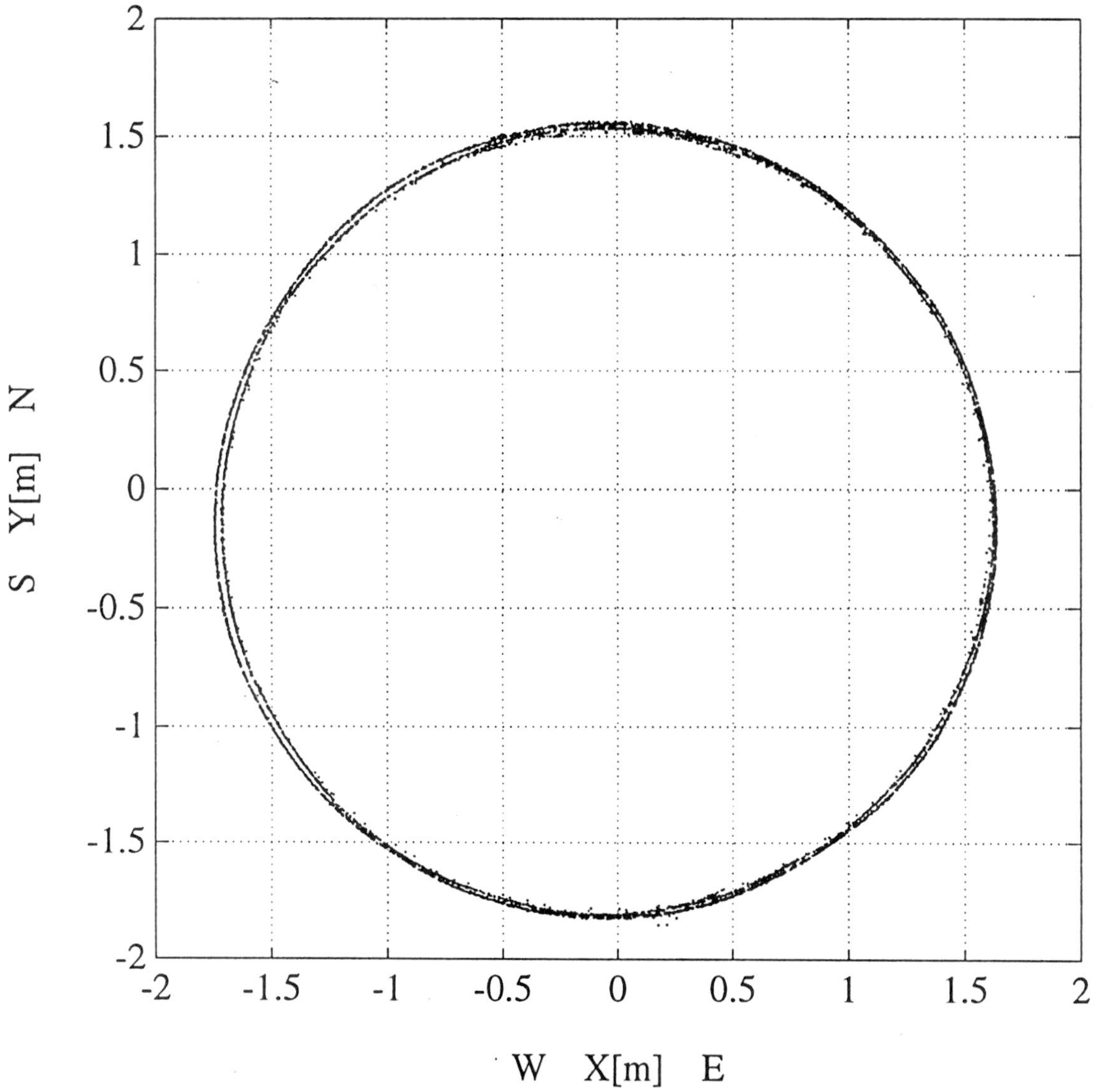

Figure A4-3 *Position solution of the first turntable test (entire dataset)*

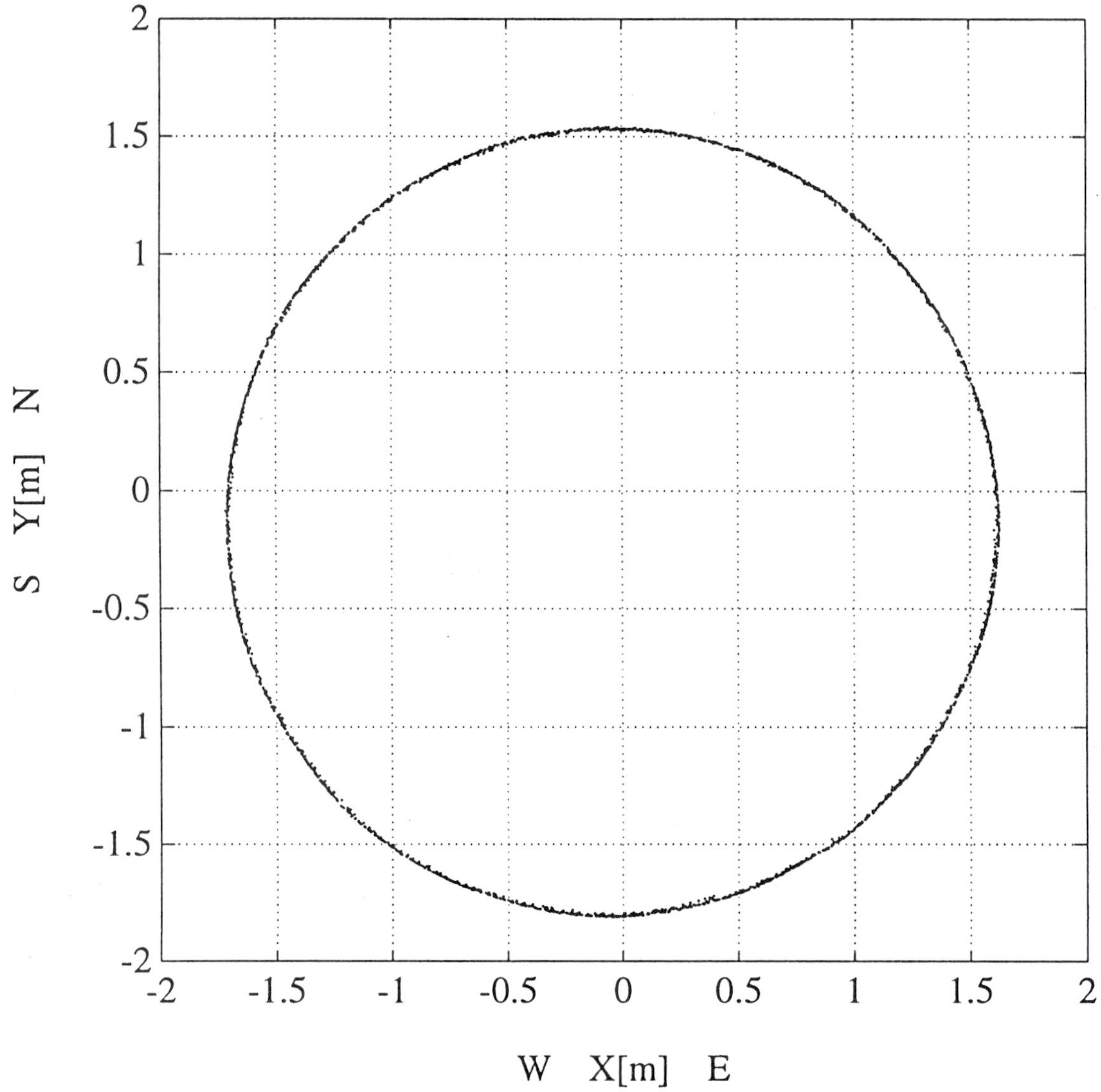

Figure A4-4 *Position solution of the first turntable test (receiver operating within specifications)*

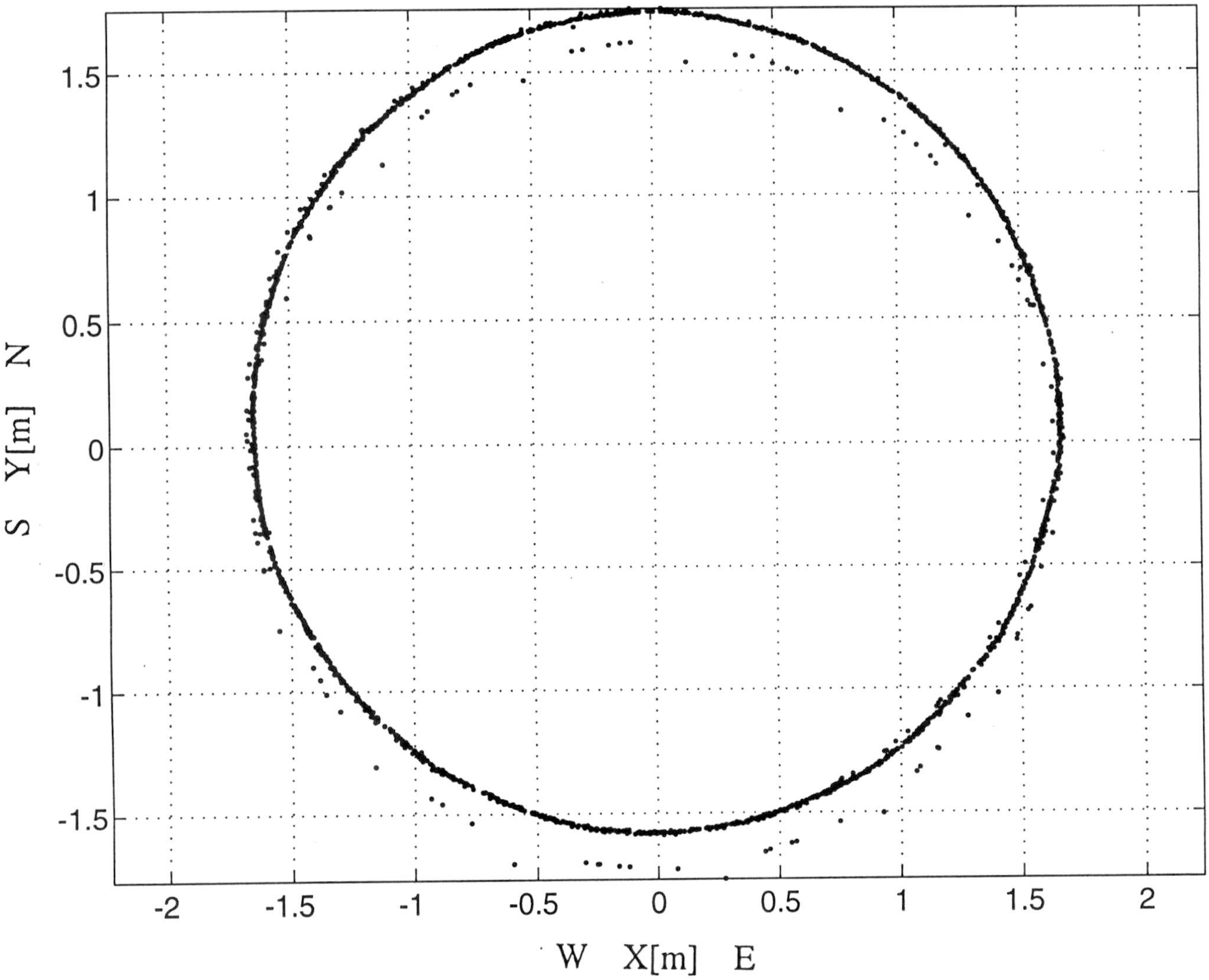

Figure A4-5 *Position solution of the second turntable test, using the reference antenna on the roof of the Electrical Engineering building*

Appendix 5 Geotracer output file of the first turntable test

```
-----------------------------------------------------------
| Geotronics kinematic postprocessing module Version 2.0    |
-----------------------------------------------------------


Running Sat Aug 10 21:35:17 1996


.\project.ini configuration:
--------------------------
Interval:    0.00
Elevation: 0
Start Time: 402008
End Time: 403101
Processing Mode: On-the-Fly
Orbit Type: Broadcast
Carrier Phase Type: L1
Maximum relative ionospheric noise:  80.0
Maximum position sigma: 20.00
Minimum ratio:   2.0
Instrument Height Corrections: trimble ext_comp_l12 625 914 69 69
Instrument Height Corrections: trimble ext_comp_l12_gp 625 2330 69 69
Instrument Height Corrections: trimble ext_geodetic_l12 692 2330 95 95
Instrument Height Corrections: trimble ext_kinematic 692 0 95 95
Instrument Height Corrections: trimble ext_geodetic 660 2330 95 95
Instrument Height Corrections: trimble ext_unknown 692 2330 95 95
Instrument Height Corrections: trimble 4000SLD 500 2415 60 70
Instrument Height Corrections: trimble 4000SX_MICRO 480 3030 80 90
Instrument Height Corrections: trimble 4000ST 600 2335 80 100
Instrument Height Corrections: ashtech Geodetic 600 1120 40 40
Instrument Height Corrections: turbo_rogue dorne_margolin_b 110 1755 780 960
Instrument Height Corrections: turbo_rogue dorne_margolin_r 60 1905 780 960
Instrument Height Corrections: turbo_rogue dorne_margolin_t 350 1905 750 930
Instrument Height Corrections: geotracer Internal 820 1120 0 0
Instrument Height Corrections: novatel Standard 410 0 0 0
Tropospheric Scaling: 0
Reference Satellite: 0
Position Output: tsat
Edit Multiplier: 3.5
Activating Lc if longer than:  10
Time Zone Offset: 2
Daylight Saving: 0
Reference Satellite Control: 30 3
Force Ambiguity Fixing: 0
Stateplane: *_not_scanned_* DEFAULT_DATUM_WGS_84
Probability Limits: 95 99.99
Systematic Errors: 1 0.1



Command line configuration:
--------------------------

--------- reference file ----------
File/Point/Info         : DLOG221A.OBS / ref_ant_ /
Rcv-type/version/serial: NovAtel GPSCard      / 7xx  9xx   /
Geocentric Position    :  3923665.565    300075.378    5002846.082 <--- DBS
Instr. Eccentricities  :        0.000         0.000          0.000
Geoid Height           :        0.000
GPS week/start/end     :          865    402008.400    403101.200
```

```
Date/start/end          :      8.8.1996    17:40:08.40    17:58:21.20
Interval                :         0.087
Code Indicators         : P1
Carrier Indicators      : P1
Mode                    : static

Sv's tracked
------------
  4  10929
  7  10929
 14  10929
 18  10929
 24    535
 25   8705
 29  10929

-------- observation file ----------
File/Point/Info         : MLOG221A.OBS / mov_ant_ /
Rcv-type/version/serial: NovAtel GPSCard      / 7xx  9xx   /
Geocentric Position     :  3923667.257    300077.044    5002844.664
Instr. Eccentricities   :         0.000         0.000          0.000
Geoid Height            :         0.000
GPS week/start/end      :           865    402008.400     403101.200
Date/start/end          :      8.8.1996    17:40:08.40    17:58:21.20
Interval                :         0.087
Code Indicators         : P1
Carrier Indicators      : P1
Mode                    : kinematic

Sv's tracked
------------
  4  10930
  7   9803
 14  10930
 15   7315
 18  10930
 24   8931
 25   9905
 29  10930


Processing in "OTF" mode
Using L1 observations for ambiguity search


Reference satellite 29, 67.7 <= elevation <= 72.6 deg

Sv's tracked simultaneously:

       sat   tracked   lli min  max.elevation
        4     10926      1 41.9 49.2
        7      9799    177 22.6 29.1
       14     10926      1 46.7 54.4
       18     10926      1 45.8 54.7
       24       483      8 13.9 14.3
       25      7678    145 15.4 18.7
       29     10926      1 67.7 72.6


Code positioning: 10927 positions of 10927 epochs (100.0 %)

402749.90 (17:52:29.90): Cycle Slip detected for satellite 25
       code - carrier triple difference: 2.34 m (3.72881 sigma)
402768.20 (17:52:48.20): Cycle Slip detected for satellite 7
       code - carrier triple difference: 2.23 m (4.09016 sigma)
402800.80 (17:53:20.80): Cycle Slip detected for satellite 25
       code - carrier triple difference: 2.73 m (4.34771 sigma)
```

```
402805.60 (17:53:25.60): Cycle Slip detected for satellite 7
      code - carrier triple difference: 3.33 m (6.10665 sigma)
402810.70 (17:53:30.70): Cycle Slip detected for satellite 7
      code - carrier triple difference: 4.58 m (8.41395 sigma)
402812.80 (17:53:32.80): Cycle Slip detected for satellite 7
      code - carrier triple difference: 7.07 m (13.0337 sigma)
402822.60 (17:53:42.60): Cycle Slip detected for satellite 7
      code - carrier triple difference: 5.80 m (10.7813 sigma)
402824.20 (17:53:44.20): Cycle Slip detected for satellite 7
      code - carrier triple difference: 5.78 m (10.8112 sigma)
402827.10 (17:53:47.10): Cycle Slip detected for satellite 7
      code - carrier triple difference: 4.26 m (8.02839 sigma)
402844.40 (17:54:04.40): Cycle Slip detected for satellite 25
      code - carrier triple difference: 4.28 m (6.82963 sigma)
402854.60 (17:54:14.60): Cycle Slip detected for satellite 25
      code - carrier triple difference: 3.93 m (6.28843 sigma)
402870.70 (17:54:30.70): Cycle Slip detected for satellite 25
      code - carrier triple difference: 4.58 m (7.35404 sigma)
402877.80 (17:54:37.80): Cycle Slip detected for satellite 7
      code - carrier triple difference: 3.88 m (7.32466 sigma)
402882.60 (17:54:42.60): Cycle Slip detected for satellite 7
      code - carrier triple difference: 2.46 m (4.6524 sigma)
402889.40 (17:54:49.40): Cycle Slip detected for satellite 25
      code - carrier triple difference: 5.11 m (8.23064 sigma)
402913.00 (17:55:13.00): Cycle Slip detected for satellite 25
      code - carrier triple difference: 8.00 m (12.9327 sigma)
402946.00 (17:55:46.00): Cycle Slip detected for satellite 25
      code - carrier triple difference: 2.94 m (4.81009 sigma)
402948.20 (17:55:48.20): Cycle Slip detected for satellite 25
      code - carrier triple difference: 9.23 m (15.1063 sigma)
402951.60 (17:55:51.60): Cycle Slip detected for satellite 7
      code - carrier triple difference: 5.82 m (11.0343 sigma)
402957.30 (17:55:57.30): Cycle Slip detected for satellite 7
      code - carrier triple difference: 10.64 m (20.3119 sigma)
402961.70 (17:56:01.70): Cycle Slip detected for satellite 25
      code - carrier triple difference: 11.09 m (18.4385 sigma)
402979.90 (17:56:19.90): Cycle Slip detected for satellite 25
      code - carrier triple difference: 6.40 m (10.887 sigma)
402983.00 (17:56:23.00): Cycle Slip detected for satellite 25
      code - carrier triple difference: 2.89 m (4.9615 sigma)
402987.10 (17:56:27.10): Cycle Slip detected for satellite 25
      code - carrier triple difference: 2.81 m (4.83271 sigma)
402987.80 (17:56:27.80): Cycle Slip detected for satellite 7
      code - carrier triple difference: 4.70 m (9.17551 sigma)
403002.70 (17:56:42.70): Cycle Slip detected for satellite 25
      code - carrier triple difference: 3.70 m (6.35922 sigma)
403004.10 (17:56:44.10): Cycle Slip detected for satellite 25
      code - carrier triple difference: 2.80 m (4.82958 sigma)
403034.60 (17:57:14.60): Cycle Slip detected for satellite 25
      code - carrier triple difference: 3.59 m (6.2074 sigma)
403049.50 (17:57:29.50): Cycle Slip detected for satellite 24
      code - carrier triple difference: 2.85 m (4.64039 sigma)
403049.70 (17:57:29.70): Cycle Slip detected for satellite 24
      code - carrier triple difference: 2.41 m (4.01371 sigma)
403050.30 (17:57:30.30): Cycle Slip detected for satellite 7
      code - carrier triple difference: 10.51 m (20.5949 sigma)
403050.50 (17:57:30.50): Cycle Slip detected for satellite 25
      code - carrier triple difference: 3.59 m (6.2193 sigma)
403051.10 (17:57:31.10): Cycle Slip detected for satellite 24
      code - carrier triple difference: 2.97 m (5.02185 sigma)
403051.40 (17:57:31.40): Cycle Slip detected for satellite 24
      code - carrier triple difference: 2.02 m (3.50448 sigma)
403068.60 (17:57:48.60): Cycle Slip detected for satellite 7
      code - carrier triple difference: 2.71 m (5.42266 sigma)
402784.00 (17:53:04.00): Cycle Slip detected for satellite 25
      code - carrier triple difference: 2.04 m (3.54137 sigma)
402867.50 (17:54:27.50): Cycle Slip detected for satellite 25
```

```
      code - carrier triple difference: 2.14 m (3.72522 sigma)
402936.20 (17:55:36.20): Cycle Slip detected for satellite 25
      code - carrier triple difference: 2.05 m (3.5656 sigma)
Deleting fragmented data, sat 24 403048...403067, 17:57:27.80...17:57:47.40
Deleting fragmented data, sat  7 402748...403069, 17:52:27.80...17:57:48.50
Deleting fragmented data, sat 25 402750...403071, 17:52:29.80...17:57:50.60

Intervals to process:

 GPS secs  Time start      secs            4  7 14 18 24 25
 402008.40 (17:40:08.40)   222             =  =  =  =
 402230.80 (17:43:50.80)   489             #  #  #  #     =
 402719.70 (17:51:59.70)     3             #     #  #     #
 402722.70 (17:52:02.70)    25             #  =  #  #     #
 402747.70 (17:52:27.70)     1             #     #  #     #
 402748.70 (17:52:28.70)   319             #     #  #
 403068.00 (17:57:48.00)     1             #     #  #  =
 403068.60 (17:57:48.60)     3             #  =  #  #  #
 403071.50 (17:57:51.50)    30             #  #  #  #  #  =

-------------------------------------------------------
Processing interval 402230.80 ... 402719.60, 488.8 secs
      6 Satellites: R29 7 4 25 18 14

Quality control:
L1 after estimate residuals:

      sv     start      end        mean slope
      14:     1.1 mm     0.7 mm     0.9 -0.00082025 mm/s
      18:     1.2 mm     1.0 mm     1.1 -0.00046952 mm/s
      25:    -0.2 mm     0.0 mm    -0.1  0.00037945 mm/s
       4:     0.6 mm     0.4 mm     0.5 -0.00042032 mm/s
       7:    -1.0 mm    -0.8 mm    -0.9  0.00056307 mm/s
      29:    -1.8 mm    -1.4 mm    -1.6  0.00076757 mm/s

    Maximum     1.8 mm <= 45.0 mm
    Max.mean    1.6 mm <= 15.0 mm
    RMS         1.0 mm <= 30.0 mm
    Slope       0.000767574 mm/s <= 1 mm/s

    L1 ambiguity determination ratio = 78.0288 > 2, ambiguities accepted

      sat  ambiguity    from        until       from        until
      14        663     402008.40   403101.00 17:40:08.40 17:58:21.00
      18       1098     402008.40   403101.00 17:40:08.40 17:58:21.00
      25       -506     402230.80   402748.60 17:43:50.80 17:52:28.60
       4        -96     402008.40   403101.00 17:40:08.40 17:58:21.00
       7       1485     402008.40   402719.60 17:40:08.40 17:51:59.60

-------------------------------------------------------
Processing interval 402722.70 ... 402747.60, 24.9 secs
      6 Satellites: R29 7 4 25 18 14
    Already known ambiguities:
      4 -96
      14 663
      18 1098
      25 -506

    L1 ambiguity determination ratio = 1.06777 <= 2, ambiguities not fixed


====================================
processing positions:
```

from to	secs	from to	fr	npos	nsat	bad	pdop	bad	badsig
402008.4-402230.7	222.3	17:40:08-17:43:50	L1	1088	5	0	5.8	0	1136
402230.8-402719.6	488.8	17:43:50-17:51:59	L1	4818	6	0	2.6	0	71
402719.7-402722.6	2.9	17:51:59-17:52:02	L1	27	5	0	3.5	0	3
402722.7-402747.6	24.9	17:52:02-17:52:27	L1	184	5	0	3.5	0	66
402747.7-402748.6	0.9	17:52:27-17:52:28	L1	0	5	0	3.5	0	10
402748.7-403067.9	319.2	17:52:28-17:57:47	L1	3193	4	0	7.2	0	0
403068.0-403068.5	0.5	17:57:48-17:57:48	L1	6	4	0	7.0	0	0
403068.6-403071.4	2.8	17:57:48-17:57:51	L1	29	4	0	7.0	0	0
403071.5-403101.0	29.5	17:57:51-17:58:21	L1	296	4	0	7.0	0	0

----

final statistics:

sv	num.obs.	RMS [mm]	min.elev.	max.elev.
4	7403	32.7	41.9	49.2
7	7113	3.4	25.0	29.1
14	7403	89.4	46.7	54.4
18	7403	18.5	45.8	54.7
25	5179	37.4	16.8	18.7
29	7403	73.0	67.7	72.6

Cycle slip summary:

7	402722.70	17:52:02.70	0	L1 not recovered
24	403068.00	17:57:48.00	0	L1 not recovered
7	403068.60	17:57:48.60	0	L1 not recovered
25	403071.50	17:57:51.50	0	L1 not recovered

Appendix 6 Geotracer output file of the second turntable test

```
---------------------------------------------------------
| Geotronics kinematic postprocessing module Version 2.0  |
---------------------------------------------------------


Running Tue Sep 17 20:17:48 1996


.\project.ini configuration:
-------------------------
Interval:     0.00
Elevation: 0
Start Time: 209220
End Time: 210120
Processing Mode: On-the-Fly
Orbit Type: Broadcast
Carrier Phase Type: L1
Maximum relative ionospheric noise:  80.0
Maximum position sigma: 20.00
Minimum ratio:   2.0
Instrument Height Corrections: trimble ext_comp_l12 625 914 69 69
Instrument Height Corrections: trimble ext_comp_l12_gp 625 2330 69 69
Instrument Height Corrections: trimble ext_geodetic_l12 692 2330 95 95
Instrument Height Corrections: trimble ext_kinematic 692 0 95 95
Instrument Height Corrections: trimble ext_geodetic 660 2330 95 95
Instrument Height Corrections: trimble ext_unknown 692 2330 95 95
Instrument Height Corrections: trimble 4000SLD 500 2415 60 70
Instrument Height Corrections: trimble 4000SX_MICRO 480 3030 80 90
Instrument Height Corrections: trimble 4000ST 600 2335 80 100
Instrument Height Corrections: ashtech Geodetic 600 1120 40 40
Instrument Height Corrections: turbo_rogue dorne_margolin_b 110 1755 780 960
Instrument Height Corrections: turbo_rogue dorne_margolin_r 60 1905 780 960
Instrument Height Corrections: turbo_rogue dorne_margolin_t 350 1905 750 930
Instrument Height Corrections: geotracer Internal 820 1120 0 0
Instrument Height Corrections: novatel Standard 410 0 0 0
Tropospheric Scaling: 0
Reference Satellite: 0
Position Output: tsat
Edit Multiplier: 3.5
Activating Lc if longer than:  10
Time Zone Offset: 2
Daylight Saving: 0
Reference Satellite Control: 30 3
Force Ambiguity Fixing: 0
Stateplane: *_not_scanned_* DEFAULT_DATUM_WGS_84
Probability Limits: 95 99.99
Systematic Errors: 1 0.1



Command line configuration:
-------------------------

--------- reference file ----------
File/Point/Info         : ELEK261A.OBS / ELEKTRO_ /
Rcv-type/version/serial: NovAtel GPSCard      / 7xx  9xx   /
Geocentric Position     :  3923665.730    300075.391    5002846.294 <--- DBS
Instr. Eccentricities   :        0.000         0.000          0.000
Geoid Height            :        0.000
GPS week/start/end      :          871    207046.700     210562.900
Date/start/end          :    17.9.1996   11:30:46.70    12:29:22.90
Interval                :        0.094
```

```
Code Indicators         : P1
Carrier Indicators      : P1
Mode                    : static

Sv's tracked
------------
  1  35029
  2  35029
  3  10210
  7  25383
 14  35029
 15  35029
 21  24176
 29  11529
 31  35029

-------- observation file ----------
File/Point/Info          : FIEL261A.OBS / FIELD_PC /
Rcv-type/version/serial: NovAtel GPSCard       / 7xx  9xx   /
Geocentric Position      :  3923689.502    300077.938    5002835.787
Instr. Eccentricities    :        0.000         0.000          0.000
Geoid Height             :        0.000
GPS week/start/end       :          871    209205.400     210309.900
Date/start/end           :    17.9.1996   12:06:45.40    12:25:09.90
Interval                 :        0.094
Code Indicators          : P1
Carrier Indicators       : P1
Mode                     : kinematic

Sv's tracked
------------
  1   5920
  2   9567
  7   9819
  9   3230
 14  10442
 15  10465
 21   8990
 25    974
 29   9676
 31   9728


Processing in "OTF" mode
Using L1 observations for ambiguity search


Reference satellite 15, 83.9 <= elevation <= 86.3 deg

Sv's tracked simultaneously:

       sat   tracked   lli min  max.elevation
        1       5756     2 31.7 33.8
        2       7630   134 16.2 19.2
        7       7880    91 19.5 25.0
       14       8503     3 45.3 52.3
       15       8526     1 83.9 86.3
       21       2301    27  6.1  7.7
       29       5892   113 12.9 18.0
       31       7789   106 26.2 33.2


Code positioning: 8160 positions of 8527 epochs (95.7 %)

209587.10 (12:13:07.10): Cycle Slip detected for satellite 7
      code - carrier triple difference: 2.13 m (5.03146 sigma)
209727.00 (12:15:27.00): Cycle Slip detected for satellite 29
      code - carrier triple difference: 2.97 m (4.91986 sigma)
209727.90 (12:15:27.90): Cycle Slip detected for satellite 29
```

```
      code - carrier triple difference: 3.05 m (5.04957 sigma)
209729.00 (12:15:29.00): Cycle Slip detected for satellite 29
      code - carrier triple difference: 2.87 m (4.76945 sigma)
209729.40 (12:15:29.40): Cycle Slip detected for satellite 29
      code - carrier triple difference: 2.84 m (4.72627 sigma)
209777.50 (12:16:17.50): Cycle Slip detected for satellite 29
      code - carrier triple difference: 2.10 m (3.50163 sigma)
209836.20 (12:17:16.20): Cycle Slip detected for satellite 31
      code - carrier triple difference: 2.28 m (6.00178 sigma)
209839.90 (12:17:19.90): Cycle Slip detected for satellite 31
      code - carrier triple difference: 2.52 m (6.63417 sigma)
209840.10 (12:17:20.10): Cycle Slip detected for satellite 7
      code - carrier triple difference: 6.54 m (15.494 sigma)
209841.00 (12:17:21.00): Cycle Slip detected for satellite 29
      code - carrier triple difference: 7.33 m (12.2338 sigma)
209843.80 (12:17:23.80): Cycle Slip detected for satellite 31
      code - carrier triple difference: 3.49 m (9.23414 sigma)
209844.00 (12:17:24.00): Cycle Slip detected for satellite 7
      code - carrier triple difference: 5.68 m (13.6643 sigma)
209852.70 (12:17:32.70): Cycle Slip detected for satellite 2
      code - carrier triple difference: 3.05 m (5.66916 sigma)
209854.80 (12:17:34.80): Cycle Slip detected for satellite 2
      code - carrier triple difference: 9.24 m (17.1999 sigma)
209857.30 (12:17:37.30): Cycle Slip detected for satellite 2
      code - carrier triple difference: 7.20 m (13.685 sigma)
209861.20 (12:17:41.20): Cycle Slip detected for satellite 7
      code - carrier triple difference: 2.34 m (5.70046 sigma)
209862.20 (12:17:42.20): Cycle Slip detected for satellite 29
      code - carrier triple difference: 6.45 m (10.9122 sigma)
209871.80 (12:17:51.80): Cycle Slip detected for satellite 7
      code - carrier triple difference: 6.09 m (14.8431 sigma)
209875.20 (12:17:55.20): Cycle Slip detected for satellite 7
      code - carrier triple difference: 7.16 m (17.7167 sigma)
209877.20 (12:17:57.20): Cycle Slip detected for satellite 31
      code - carrier triple difference: 2.13 m (5.65809 sigma)
209877.20 (12:17:57.20): Cycle Slip detected for satellite 7
      code - carrier triple difference: 2.84 m (7.17479 sigma)
209878.30 (12:17:58.30): Cycle Slip detected for satellite 7
      code - carrier triple difference: 8.68 m (21.9936 sigma)
209880.20 (12:18:00.20): Cycle Slip detected for satellite 2
      code - carrier triple difference: 3.65 m (7.02899 sigma)
209880.60 (12:18:00.60): Cycle Slip detected for satellite 2
      code - carrier triple difference: 2.68 m (5.16483 sigma)
209892.60 (12:18:12.60): Cycle Slip detected for satellite 31
      code - carrier triple difference: 2.14 m (5.69404 sigma)
209898.10 (12:18:18.10): Cycle Slip detected for satellite 31
      code - carrier triple difference: 3.52 m (9.392 sigma)
209899.80 (12:18:19.80): Cycle Slip detected for satellite 7
      code - carrier triple difference: 3.68 m (9.62638 sigma)
209901.40 (12:18:21.40): Cycle Slip detected for satellite 7
      code - carrier triple difference: 4.34 m (11.4268 sigma)
209903.70 (12:18:23.70): Cycle Slip detected for satellite 2
      code - carrier triple difference: 3.65 m (7.05757 sigma)
209908.10 (12:18:28.10): Cycle Slip detected for satellite 2
      code - carrier triple difference: 2.78 m (5.38699 sigma)
209909.40 (12:18:29.40): Cycle Slip detected for satellite 2
      code - carrier triple difference: 2.90 m (5.6372 sigma)
209910.70 (12:18:30.70): Cycle Slip detected for satellite 29
      code - carrier triple difference: 4.38 m (7.48632 sigma)
209917.40 (12:18:37.40): Cycle Slip detected for satellite 7
      code - carrier triple difference: 2.12 m (5.6229 sigma)
209918.70 (12:18:38.70): Cycle Slip detected for satellite 31
      code - carrier triple difference: 2.45 m (6.58741 sigma)
209928.20 (12:18:48.20): Cycle Slip detected for satellite 2
      code - carrier triple difference: 5.01 m (9.76419 sigma)
209933.30 (12:18:53.30): Cycle Slip detected for satellite 29
      code - carrier triple difference: 7.57 m (12.9895 sigma)
209934.20 (12:18:54.20): Cycle Slip detected for satellite 2
      code - carrier triple difference: 2.64 m (5.16747 sigma)
```

```
209934.20 (12:18:54.20): Cycle Slip detected for satellite 29
      code - carrier triple difference: 2.85 m (4.96502 sigma)
209951.40 (12:19:11.40): Cycle Slip detected for satellite 2
      code - carrier triple difference: 2.20 m (4.32634 sigma)
209963.30 (12:19:23.30): Cycle Slip detected for satellite 31
      code - carrier triple difference: 2.31 m (6.21957 sigma)
209972.20 (12:19:32.20): Cycle Slip detected for satellite 31
      code - carrier triple difference: 2.91 m (7.83941 sigma)
209979.50 (12:19:39.50): Cycle Slip detected for satellite 29
      code - carrier triple difference: 2.22 m (3.88121 sigma)
209989.40 (12:19:49.40): Cycle Slip detected for satellite 2
      code - carrier triple difference: 6.57 m (12.9177 sigma)
210001.00 (12:20:01.00): Cycle Slip detected for satellite 29
      code - carrier triple difference: 5.22 m (9.13084 sigma)
210015.20 (12:20:15.20): Cycle Slip detected for satellite 7
      code - carrier triple difference: 2.19 m (5.8276 sigma)
210029.40 (12:20:29.40): Cycle Slip detected for satellite 29
      code - carrier triple difference: 5.91 m (10.4019 sigma)
210030.30 (12:20:30.30): Cycle Slip detected for satellite 2
      code - carrier triple difference: 2.24 m (4.44939 sigma)
210031.40 (12:20:31.40): Cycle Slip detected for satellite 2
      code - carrier triple difference: 2.70 m (5.36983 sigma)
210031.40 (12:20:31.40): Cycle Slip detected for satellite 29
      code - carrier triple difference: 4.35 m (7.72989 sigma)
210034.50 (12:20:34.50): Cycle Slip detected for satellite 29
      code - carrier triple difference: 2.34 m (4.17439 sigma)
210049.30 (12:20:49.30): Cycle Slip detected for satellite 2
      code - carrier triple difference: 2.93 m (5.83907 sigma)
210050.10 (12:20:50.10): Cycle Slip detected for satellite 2
      code - carrier triple difference: 3.14 m (6.26538 sigma)
210058.70 (12:20:58.70): Cycle Slip detected for satellite 2
      code - carrier triple difference: 2.31 m (4.63402 sigma)
210066.30 (12:21:06.30): Cycle Slip detected for satellite 2
      code - carrier triple difference: 2.83 m (5.67402 sigma)
209654.70 (12:14:14.70): Cycle Slip detected for satellite 29
      code - carrier triple difference: 2.08 m (3.71415 sigma)
209654.80 (12:14:14.80): Cycle Slip detected for satellite 29
      code - carrier triple difference: 2.11 m (3.77083 sigma)
Satellite 29 has only 1 epoch of data at 209655 sec (12:14:14.70)
Deleting fragmented data, sat  2 209655...209657, 12:14:15.20...12:14:17.30
Deleting fragmented data, sat 29 209726...209729, 12:15:26.20...12:15:29.20
Deleting fragmented data, sat 14 209780...209781, 12:16:20.40...12:16:20.90
Deleting fragmented data, sat 29 209776...209790, 12:16:16.30...12:16:29.90
Deleting fragmented data, sat  7 209838...210015, 12:17:18.30...12:20:15.10
Deleting fragmented data, sat 31 209835...210020, 12:17:15.40...12:20:20.30
Deleting fragmented data, sat 29 209836...210044, 12:17:15.80...12:20:44.20
Deleting fragmented data, sat  2 209836...210091, 12:17:16.20...12:21:31.20
Deleting fragmented data, sat  1 209841...209841, 12:17:20.70...12:17:21.20
Deleting fragmented data, sat 21 209401...209474, 12:10:01.00...12:11:14.10

Intervals to process:

 GPS secs  Time start      secs          1  2  7 14 21 29 31
 209220.00 (12:07:00.00)   179           =  =  =  =  =     =
 209399.20 (12:09:59.20)     8           #  #  #  #        #
 209407.40 (12:10:07.40)   178           #  #  #  #     =  #
 209585.10 (12:13:05.10)     1           #  #  #  #        #
 209586.30 (12:13:06.30)     1           #  #  #  #     =  #
 209587.10 (12:13:07.10)    68           #  #  =  #     #  #
 209654.60 (12:14:14.60)     0           #     #  #     #  #
 209654.70 (12:14:14.70)     0           #     #  #        #
 209654.80 (12:14:14.80)     3           #     #  #     =  #
 209658.10 (12:14:18.10)    68           #  =  #  #     #  #
 209726.10 (12:15:26.10)     3           #  #  #  #        #
 209729.40 (12:15:29.40)    46           #  #  #  #     =  #
 209775.70 (12:16:15.70)     4           #  #  #  #        #
 209779.50 (12:16:19.50)     3           #  #  #           #
 209782.40 (12:16:22.40)     8           #  #  #  =        #
 209790.80 (12:16:30.80)    44           #  #  #  #     =  #
```

```
209835.00 (12:17:15.00)    0          #   #   #   #           #
209835.20 (12:17:15.20)    0          #       #   #           #
209835.30 (12:17:15.30)    2          #       #   #
209837.20 (12:17:17.20)  178                      #
210015.20 (12:20:15.20)    6                  =   #
210021.00 (12:20:21.00)   24                  #   #           =
210045.20 (12:20:45.20)   47                  #   #       =   #
210092.20 (12:21:32.20)   28              =   #   #       #   #

-------------------------------------------------------
Processing interval 209407.40 ... 209585.00, 177.6 secs
      7 Satellites: R15 29 2 31 1 7 14

Quality control:
L1 after estimate residuals:

      sv    start      end        mean slope
      14:    2.3 mm   -0.7 mm     0.8 -0.01700474 mm/s
       7:   -2.3 mm   -2.2 mm    -2.3  0.00056905 mm/s
       1:    2.2 mm    0.3 mm     1.3 -0.01029289 mm/s
      31:    2.9 mm   -4.8 mm    -1.0 -0.04368238 mm/s
       2:    2.5 mm    1.6 mm     2.0 -0.00510451 mm/s
      29:   -4.0 mm    3.6 mm    -0.2  0.04320203 mm/s
      15:   -3.5 mm    2.2 mm    -0.6  0.03231343 mm/s

    Maximum     4.8 mm <= 45.0 mm
    Max.mean    2.3 mm <= 15.0 mm
    RMS         2.0 mm <= 30.0 mm
    Slope       0.043202 mm/s <= 1 mm/s

    L1 ambiguity determination ratio = 6.24547 > 2, ambiguities accepted

      sat  ambiguity    from        until       from         until
      14      -979      209220.00   209779.40   12:07:00.00  12:16:19.40
       7      -866      209220.00   209587.00   12:07:00.00  12:13:07.00
       1     -1413      209220.00   209836.90   12:07:00.00  12:17:16.90
      31     -1202      209220.00   209835.20   12:07:00.00  12:17:15.20
       2        87      209220.00   209654.50   12:07:00.00  12:14:14.50
      29     -1268      209407.40   209585.00   12:10:07.40  12:13:05.00

-------------------------------------------------------
Processing interval 209658.10 ... 209779.40, 121.3 secs
      6 Satellites: R15 2 1 7 31 14
    Already known ambiguities:
       1 -1413
      14 -979
      31 -1202

    L1 ambiguity determination ratio = 1.23049 <= 2, ambiguities not fixed

-------------------------------------------------------
Processing interval 209654.80 ... 209726.00, 71.2 secs
      6 Satellites: R15 29 1 7 31 14
    Already known ambiguities:
       1 -1413
      14 -979
      31 -1202

    L1 ambiguity determination ratio = 1.06999 <= 2, ambiguities not fixed

-------------------------------------------------------
Processing interval 209587.10 ... 209779.40, 192.3 secs
      5 Satellites: R15 7 1 31 14
    Already known ambiguities:
       1 -1413
      14 -979
      31 -1202
```

```
Quality control:
L1 after estimate residuals:

      sv    start      end        mean slope
       7:    0.7 mm    18.2 mm     9.5  0.09112031 mm/s
      15:    0.2 mm    34.2 mm    17.2  0.17713318 mm/s
       1:   -0.4 mm   -26.4 mm   -13.4 -0.13533349 mm/s
      31:    0.4 mm    26.6 mm    13.5  0.13612341 mm/s
      14:   -0.3 mm   -52.6 mm   -26.5 -0.27198536 mm/s

    Maximum    52.6 mm > 45.0 mm, ambiguities not used


-------------------------------------------------------
Processing interval 209587.10 ... 209654.60, 67.5 secs
      6 Satellites: R15 29 1 7 31 14
    Already known ambiguities:
       1 -1413
      14 -979
      31 -1202

Quality control:
L1 after estimate residuals:

      sv    start      end        mean slope
       7:  -21.5 mm     1.3 mm   -10.1  0.33789571 mm/s
      29:  -21.0 mm     5.4 mm    -7.8  0.38998221 mm/s
      15:   -8.4 mm     6.9 mm    -0.8  0.22617461 mm/s
       1:   10.0 mm    -3.5 mm     3.2 -0.20020469 mm/s
      31:   16.2 mm    -2.8 mm     6.7 -0.28162552 mm/s
      14:    0.6 mm    -7.2 mm    -3.3 -0.11515480 mm/s

    Maximum    21.5 mm <= 45.0 mm
    Max.mean   10.1 mm <= 15.0 mm
    RMS         8.2 mm <= 30.0 mm
    Slope       0.389982 mm/s <= 1 mm/s


    L1 ambiguity determination ratio = 4.53383 > 2, ambiguities accepted

      sat  ambiguity    from        until       from        until
       7        -865    209587.10   209836.90   12:13:07.10 12:17:16.90
      29       -1274    209586.30   209654.60   12:13:06.30 12:14:14.60

-------------------------------------------------------
Processing interval 209658.10 ... 209835.10, 177.0 secs
      5 Satellites: R15 2 1 7 31
    Already known ambiguities:
       1 -1413
       7 -865
      31 -1202

    L1 ambiguity determination ratio = 1.11076 <= 2, ambiguities not fixed

-------------------------------------------------------
Processing interval 209658.10 ... 209779.40, 121.3 secs
      6 Satellites: R15 2 1 7 31 14
    Already known ambiguities:
       1 -1413
       7 -865
      14 -979
      31 -1202

    L1 ambiguity determination ratio = 1.08943 <= 2, ambiguities not fixed

-------------------------------------------------------
Processing interval 209654.80 ... 209726.00, 71.2 secs
      6 Satellites: R15 29 1 7 31 14
    Already known ambiguities:
```

```
      1 -1413
      7 -865
     14 -979
     31 -1202

    L1 ambiguity determination ratio = 1.06236 <= 2, ambiguities not fixed

-------------------------------------------------------
Processing interval 209220.00 ... 209399.10, 179.1 secs
      7 Satellites: R15 21 2 31 1 7 14
    Already known ambiguities:
      1 -1413
      2 87
      7 -866
     14 -979
     31 -1202

Quality control:
L1 after estimate residuals:

      sv     start       end        mean slope
      21:     3.6 mm   14.4 mm     9.0  0.06056044 mm/s
      15:    -0.3 mm    6.6 mm     3.1  0.03848847 mm/s
       2:    -7.4 mm   -4.8 mm    -6.1  0.01421560 mm/s
      31:    -1.8 mm   -6.9 mm    -4.4 -0.02859631 mm/s
       1:    -4.8 mm  -16.8 mm   -10.8 -0.06717323 mm/s
       7:     4.5 mm   -1.9 mm     1.3 -0.03565983 mm/s
      14:     6.2 mm    9.4 mm     7.8  0.01816487 mm/s

    Maximum   16.8 mm <= 45.0 mm
    Max.mean  10.8 mm <= 15.0 mm
    RMS        7.2 mm <= 30.0 mm
    Slope      0.0605604 mm/s <= 1 mm/s


    L1 ambiguity determination ratio = 11.1603 > 2, ambiguities accepted

      sat  ambiguity    from       until      from        until
      21       -471     209220.00  209399.10 12:07:00.00 12:09:59.10

-------------------------------------------------------
Processing interval 209658.10 ... 209726.00, 67.9 secs
      7 Satellites: R15 29 2 31 1 7 14
    Already known ambiguities:
      1 -1413
      7 -865
     14 -979
     31 -1202

    L1 ambiguity determination ratio = 1.51089 <= 2, ambiguities not fixed

-------------------------------------------------------
Processing interval 209729.40 ... 209775.60, 46.2 secs
      7 Satellites: R15 29 2 31 1 7 14
    Already known ambiguities:
      1 -1413
      7 -865
     14 -979
     31 -1202

    L1 ambiguity determination ratio = 1.11328 <= 2, ambiguities not fixed

-------------------------------------------------------
Processing interval 210045.20 ... 210120.00, 74.8 secs
      5 Satellites: R15 29 7 14 31

    L1 ambiguity determination ratio = 1.01943 <= 2, ambiguities not fixed

===================================
```

processing positions:

from to	secs	from to	fr	npos	nsat	bad	pdop	bad	badsig
209220.0-209399.1	179.1	12:07:00-12:09:59	L1	1773	7	0	1.9	0	10
209399.2-209407.3	8.1	12:09:59-12:10:07	L1	70	6	0	2.3	0	0
209407.4-209585.0	177.6	12:10:07-12:13:05	L1	1469	7	0	1.9	0	43
209585.1-209586.2	1.1	12:13:05-12:13:06	L1	12	6	0	2.2	0	0
209586.3-209587.0	0.7	12:13:06-12:13:07	L1	4	7	0	1.9	0	4
209587.1-209654.5	67.4	12:13:07-12:14:14	L1	584	7	0	1.9	0	81
209654.6-209654.6	0.0	12:14:14-12:14:14	L1	0	6	0	2.0	0	1
209654.7-209654.7	0.0	12:14:14-12:14:14	L1	0	5	0	2.4	0	1
209654.8-209658.0	3.2	12:14:14-12:14:18	L1	0	5	0	2.4	0	33
209658.1-209726.0	67.9	12:14:18-12:15:26	L1	0	5	0	2.4	0	663
209726.1-209729.2	3.1	12:15:26-12:15:29	L1	0	5	0	2.4	0	29
209729.4-209775.6	46.2	12:15:29-12:16:15	L1	4	5	0	2.4	0	431
209775.7-209779.4	3.7	12:16:15-12:16:19	L1	23	5	0	2.4	0	15
209779.5-209782.3	2.8	12:16:19-12:16:22	L1	29	4	0	2.6	0	0
209782.4-209790.5	8.1	12:16:22-12:16:30	L1	82	4	0	2.6	0	0
209790.8-209834.9	44.1	12:16:30-12:17:14	L1	370	4	0	2.6	0	0
209835.0-209835.1	0.1	12:17:15-12:17:15	L1	2	4	0	2.6	0	0
209835.2-209835.2	0.0	12:17:15-12:17:15	L1	1	4	0	2.6	0	0
209835.3-209836.9	1.6	12:17:15-12:17:16		0	3				
209837.2-210015.1	177.9	12:17:17-12:20:15		0	0				
210015.2-210020.9	5.7	12:20:15-12:20:20		0	0				
210021.0-210045.1	24.1	12:20:21-12:20:45		0	0				
210045.2-210092.1	46.9	12:20:45-12:21:32		0	0				
210092.2-210120.0	27.8	12:21:32-12:22:00		0	0				

----

final statistics:

sv	num.obs.	RMS [mm]	min.elev.	max.elev.
1	5250	37.7	31.7	33.8
2	4050	62.7	17.9	19.2
7	5250	52.9	19.5	23.3
14	5250	29.7	45.3	49.6
15	5250	23.0	83.9	86.3
21	1783	49.7	6.6	7.7
29	2186	22.6	12.9	14.6
31	5250	19.2	28.4	33.2

Cycle slip summary:

29	209586.30	12:13:06.30	-6	L1	recovered
7	209587.10	12:13:07.10	1	L1	recovered
29	209654.80	12:14:14.80	0	L1	not recovered
2	209658.10	12:14:18.10	0	L1	not recovered
29	209729.40	12:15:29.40	0	L1	not recovered
14	209782.40	12:16:22.40	0	L1	not recovered
29	209790.80	12:16:30.80	0	L1	not recovered
7	210015.20	12:20:15.20	0	L1	not recovered
31	210021.00	12:20:21.00	0	L1	not recovered
29	210045.20	12:20:45.20	0	L1	not recovered
2	210092.20	12:21:32.20	0	L1	not recovered